Induction Heating of Aluminum Cookware

Andrew Aloysius Amrhein

Thesis submitted to the faculty of the Virginia Polytechnic Institute and State University in partial fulfillment of the requirements for the degree of

Master of Science
In
Electrical Engineering

Committee:
Jih S. (Jason) Lai
Jaime De La Reelopez
Daniel M. Sable

May 21, 2015
Blacksburg, VA

Keywords:
All-Metal Induction Cooker, High-Frequency Skin Effect, Low-Resistivity Induction Heating, Series-Load-Resonant, Soft-Switching Inverter, Transformer Impedance Matching

Induction Heating of Aluminum Cookware

Andrew Aloysius Amrhein

ABSTRACT

Induction heating has become a popular alternative to other heat sources for stovetop cooking applications due to performance, efficiency, control response, and safety. The main drawback is that extreme difficulty is encountered when trying to head low-resistivity, non-ferromagnetic metals such as aluminum and copper, which are commonly used for cookware in several societies. The lack of ferromagnetic properties, resulting in no hysteresis dissipation, and low resistivity of such metals results in an impractically low resistance reflected through the work coil. The resultant impedance complicates inverter design, as it is too low to be efficiently driven with conventional inverter topologies. The magnitudes of current involved in exciting this impedance also severely impact the efficiency of the coil and resonant components, requiring extreme care in coil design. This work explores various techniques that have been proposed and/or applied to efficiently heat low-resistivity cookware and the associated limitations. A transformer-coupled series-load-resonant topology driven by a full-bridge inverter is proposed as a means of efficiently heating aluminum cookware within practical design constraints. The experimental circuit is built and successfully tested at an output power of 1.66kW. The procedure of optimizing the work coil for improved efficiency is also presented along with the procedure of measuring coil efficiency. An improved circuit incorporating switch voltage detection to guarantee zero-voltage switching is then built in order to overcome limitations of this design.

CONTENTS

LIST OF FIGURES

LIST OF TABLES

I. INTRODUCTION

In recent years, induction cooking devices have become increasingly popular alternatives to conventional cooking methods due to efficiency, safety, and heating performance [1]. One of the drawbacks though is that induction heating performance is dependent on the material of the cookware and most products currently available aren't compatible with aluminum cookware. This becomes a problem in that a significant portion of the pots and pans on the market are currently made of aluminum as it offers low manufacturing cost and has superior thermal performance to iron and stainless steel. The very few aluminum-compatible induction cookers on the market are very costly and not highly efficient.

Induction heating involves resistive heating of a material by eddy currents induced by magnetic coupling with a work coil that is driven with a high-frequency alternating current. In ferromagnetic materials, the alternating magnetic fields result in hysteresis heating, which contributes to the heating effect. The problem with aluminum and copper is that their resistivity is significantly lower than that of iron or stainless steel. This requires much larger magnitudes of induced currents to deliver a specified amount of power. In addition, there is no additional hysteresis heating due to the lack of ferromagnetic properties and therefore all heating must be carried out by induced eddy currents. The required magnitude of induced currents not only complicates the design of an efficient coil, but is impractical for inverter design. Another challenge is that the large magnitudes of induced eddy currents can interact with the high magnitudes of flux from the work coil and create repulsive Lorentz forces potentially capable of lifting or moving the pan off the cooker, an undesirable effect.

Several techniques have been applied to the development of an all-metal induction cooker, both in literature and industry, with varying degrees of success and each with its own

limitations. Increasing the number of turns in the work coil is a straightforward means of increasing the reflected resistance seen at the terminals. However, increased turns results in increased AC losses and high resonant voltages. Increasing the operating frequency increases the effective resistance of the cooking vessel due to skin effect, but also results in increased coil and inverter losses. Inverters have been specifically designed for high-frequency operation for this task, such as in [2], but performance was restricted due to circuit limitations. Various topologies, such as the single-ended, multi-resonant frequency doubler, have also been developed to allow for the work coil to be driven at frequencies higher than the switching frequency, allowing for operation above efficient switching frequency limits. A novel topology that allows for the coil to be driven at twice the switching frequency while still allowing for soft-switching conditions to be maintained over a wide power control range is presented in [3] and [4]. An induction coil consisting of two windings driven out-of phase is presented in [5] as a means of operating with an effective frequency higher than the electronic circuit is actually delivering. A series-resonant topology where the resonant tank is excited at an odd harmonic of the switching frequency is presented in [6][7][8][9] in different permutations. In addition to allowing for higher operating frequency, this harmonic technique also results in an effective voltage step-down ratio, allowing for matching to the low coil resistance. The limitation to this is that it involves additional circulating energy and losses. Other methods of matching the reflected coil impedance to the inverter output include L-C matching networks and transformer matching; both of which are used in various industrial applications but are previously avoided in cooking devices. Devices have also been patented, such as [10], which focus the magnetic flux from the coil to a smaller area of the cooking vessel in order to increase the effective resistance

of the material. Although functional to this end, additional heating occurs, therefore resulting in efficiency challenges.

This paper presents a transformer-coupled, series-resonant topology as a means of efficiently heating low-resistivity metals under these conditions. The main design factor for the work coil is its efficiency at the required current levels, as the matching transformer eliminates the need for the coil to present an easy-to-drive impedance to the inverter. The series-resonant circuit consists of high-current, high-frequency capacitors in resonance with the leakage inductance of the work coil and circuit parasitics. The resonant tank is then coupled to a full-bridge inverter through a matching transformer. The circuit is operated at 120kHz to utilize some benefit from skin effect in the vessel being heated.

In addition to the proposed topology, this work also evaluates the effect of operating frequency on the performance and efficiency of heating low-resistivity, non-ferromagnetic metals. Different induction work coil designs are evaluated and their efficiency is measured as a function of frequency. An experimental circuit is also evaluated for heating aluminum cookware with a switching frequency of 1MHz.

II. LITERATURE REVIEW AND EXISTING TECHNOLOGIES

Induction Cooker Topologies and Developments

Regardless of topology, all modern and recent induction cooking designs involve some form of resonance between the work coil and additional circuit elements. This resonant configuration can be classified to be directly or some permutation of either a series-resonant (figure 2.1a) or parallel-resonant (figure 2.1b) topology.

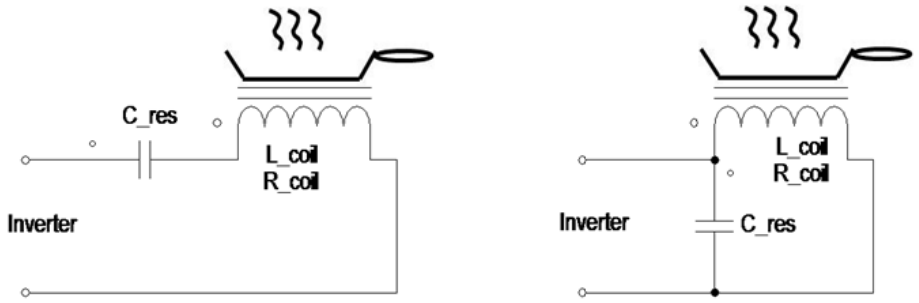

Figure 2.1 (a) Series-Resonant (left) and (b) Parallel-Resonant (right) Induction Cooker Topologies

Although several induction heating (IH) inverter topologies exist, there are three general inverter topologies that are used in the majority of induction cooking devices. The full-bridge inverter is used in both high-power, more-expensive induction cookers and in a plethora of industrial applications. The disadvantage of this topology is the number of active elements and the fact that current must flow through two switches at any given time. The half-bridge inverter [11] is also used heavily in induction cookers and industrial applications. In a half-bridge inverter the current only flows through one switch at any given time. However, switch current is higher for a given power level, increasing losses and making it less preferable for high-power applications. Both of these topologies clamp the output voltage to the DC bus voltage, preventing excessive resonant voltage from damaging the switches. The single switch topologies [12][13]

shown in figures 2.2a and 2.2b are used in a wide range of cooking and low-power industrial applications due to low-active-component count and low cost. Unlike the full- and half-bridge inverters, these single-switch designs do not offer voltage clamping and therefore present the risk of overvoltage damage to the switch in the event of improper resonant conditions. Voltage-sourced inverters, such as half- and full-bridge, are usually used to drive a series-resonant induction load. A parallel-resonant load results in the resonant capacitor connected across the inverter output, which poses problems for switching. An additional series inductor can solve this issue, but is not employed in cooking applications due to the added complexity. The parallel-resonant tank is usually driven directly by a single-switch inverter topology, which due to a current-sourced or multi-resonant nature, is much more suitable for this application.

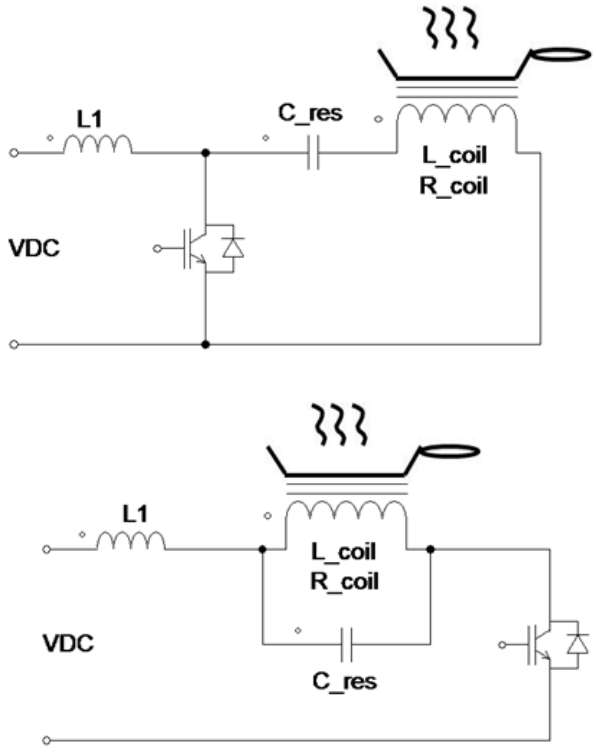

Figure 2.2 (a) Series-Resonant (top) and (b) Parallel-Resonant (bottom) Single-Switch Topologies

A few novel topologies as well as a large number of topological modifications have been proposed with improvements over these basic designs in the areas of efficiency, reliability, component requirements, and control. In domestic induction cooking devices, the main improvements were either to improve efficiency by supporting soft-switching at minimal cost or to improve power control.

Several modifications have been proposed to improve soft-switching and control capabilities of the half-bridge inverter discussed in [11]. In [14] and [15], an additional switch and capacitor are added across on switch as shown in figure 2.3. A second resonance supported by the additional branch permits for the main switches to be switched with zero-voltage and zero-current switching over a wide operating range. This allows for a greatly increased range of power control while still maintaining soft-switching. It also permits the inverter to be operated at unity power factor while still having a means to charge device capacitances to provide zero-voltage turn-on. A similar form of edge-resonant zero-voltage switching is achieved by the topology presented in [16], shown in figure 2.4. Here, an additional capacitor is added in series with the resonant tank and the auxiliary switch is used to bypass the additional capacitor. Neither of these designs are heavily used, as modern high-speed IGBTs yield less benefit from zero-current turn-off and the lower power factor required to achieve zero-voltage turn-on is considered acceptable in most domestic cooking devices.

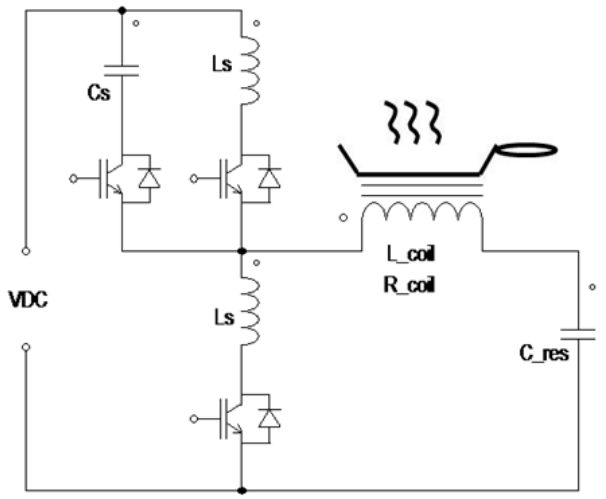

Figure 2.3 Switched-Capacitor Branch Added to HB Inverter to Support Soft-Switching

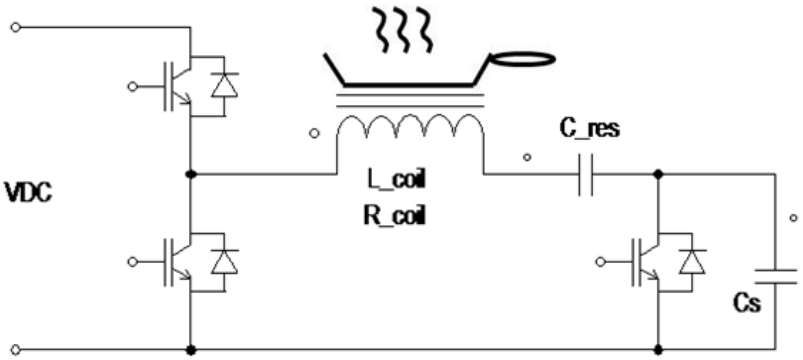

Figure 2.4 Switched Capacitor in Series with Resonant Tank to Assist with Zero-Voltage Turn-On

In order to reduce losses at reduced-power operation, [17] and [18] add additional switched snubber capacitors to the half-bridge switches as shown in figure 2.5. By adding capacitors significantly larger than the resonant capacitance across the switches, switch voltage increases much more slowly at turn-off, therefore reducing the turn-off losses. The problem with the large capacitance though is that the increased charge-time makes zero-voltage turn-on difficult to achieve without high-turn-off current and/or large dead-time. This is solved by only switching the additional snubber capacitors into the circuit at reduced power and operating without the capacitors at high power. Both [17] and [18] also switch different resonant

capacitors to adapt operating frequency and to further support the zero-derivative switching. The main disadvantage to this design is the complexity and component count. The boost-half-bridge (BHB) shown in figure 2.6, such as proposed in [19], allows for the inverter to be operated with a higher effective bus voltage than is available from the rectifier. Although the increased voltage is not necessary if the coil and resonant tank are properly designed, the variable voltage step-up allows for increased control capabilities and for the circuit to be adapted to cookware of different resistivity as well as variations in supply voltage.

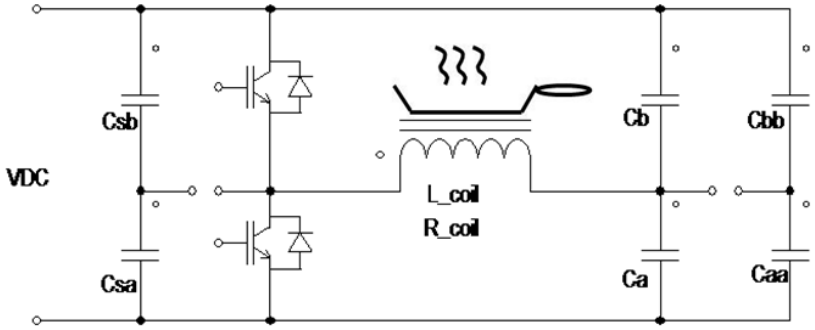

Figure 2.5 Dual-Mode Topology with Switched Snubber and Resonant Capacitors

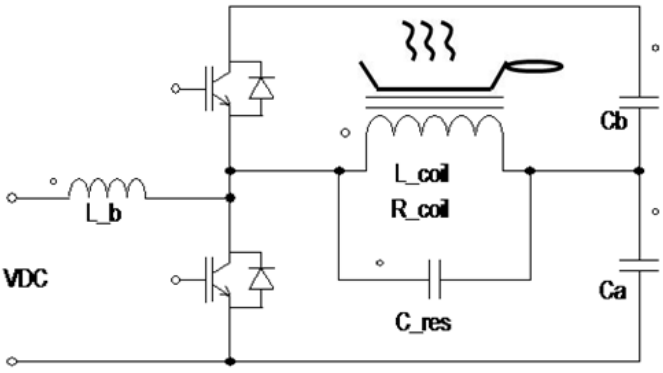

Figure 2.6 Boost-Half-Bridge (BHB) Inverter Driving Parallel-Resonant Load

A wide variety of modifications have been proposed for single-switch topologies. Although no topological modification, [20] proposes new drive schemes in order improve efficiency and control capabilities. A quasi-resonant inverter (figure 2.7) consisting of an auxiliary switch is series with the parallel resonant capacitor in a single-switch inverter is proposed in [21]. This quasi-resonant design provides zero-voltage turn-on over a wide range of the switching cycle and also clamps switch voltage spikes to some degree while only requiring one additional component (switch). A similar topology is presented in [22]. The Active-clamp modification shown in figure 2.8 adds an additional switched capacitor leg to the single-switch inverter. Although requiring an additional capacitor, this multi-resonant design yields increased efficiency over the previous quasi-resonant design and also provides voltage clamping for both switches. In a further improvement overt these two designs, the boost-active clamp single-switch inverter adds a boost inductor to the active-clamp initially-single-switch inverter as proposed in [23] and [24]. It should be noted that this topology is actually the boost-half-bridge design previously discussed. With respect to the clamped single-switch that it was derived from, this topology offers multiple advantages. The boost functionality yields higher efficiency at high power over a varying load impedance range as is characteristic of the BHB. Unlike the other clamped permutations of an initially single-switch design, there is no DC current through the work coil, further improving efficiency.

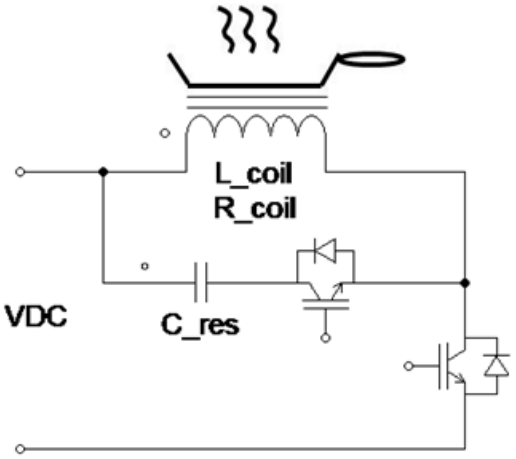

Figure 2.7 Quasi-Resonant Induction Cooker Topology

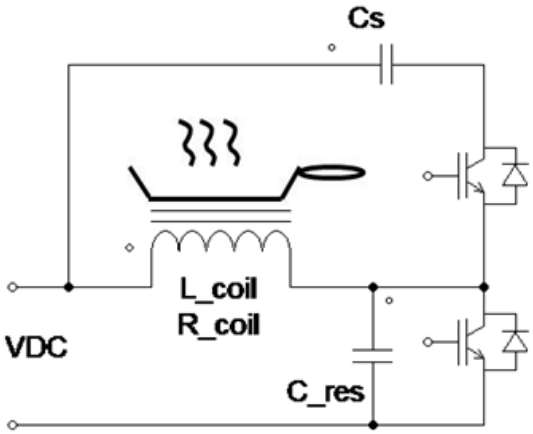

Figure 2.8 Active Clamp Added to Single-Switch IH Inverter

In order to reduce overall component count, the quasi-resonant topology shown in figure 2.7 is implemented using bi-directionally-blocking switches in [25]. This allows the circuit to operate identically regardless of supply polarity, removing the rectifier from the circuit. Each switch consists of two reverse-polarity IGBTs, with a gate signal applied to one for the entirety of the line half-cycle. Aside from limitations of the general topology itself, the disadvantage of this design is the increased control and gate drive complexity.

In most domestic induction cooker designs, the circuit is operated as natural power-factor correction (PFC) where there is no smoothing filter on the output of the front-end rectifier.

Although double-line-frequency ripple is not noticed in thermal performance, the modulation of electromagnetic forces acting between the coil and cooking vessel can create vibration and audible noise. Although not common, a smoothed DC supply is sometimes used to solve this problem. A full-bridge inverter supplied by a boost power-factor-correction rectifier is proposed in [26] and [27] to supply clean DC to the inverter while maintaining acceptable input power factor. The boost PFC also allows for the unit to adapt to variations in supply voltage. The disadvantage of this is increased complexity and the need to store energy between parts of the AC line cycle.

Low-Resistivity Induction Cooker Techniques

Although many of the above topologies yield improvements to the induction heating of ferromagnetic cookware, none of them make any notable advances in heating low-resistivity cookware. Several other designs have been proposed and implemented for the purpose of heating low-resistivity, non-ferromagnetic cookware. The challenge in developing an induction cooker compatible with low-resistivity, non-ferromagnetic metals is to provide an impedance that can be easily driven by an inverter and doing so in a practical, efficient, and cost-effective manner. There are essentially four places in the system where modification can allow for compatibility with low-resistivity metals. The effective resistance of the cooking vessel can be increased by means of skin effect. Secondly, the coil can be designed to reflect higher terminal resistance. The third option is to use additional circuitry to match the low impedance to the inverter output. Last, the inverter itself (along with the remainder of the circuit) can be designed to operate with the low impedance load.

A. Increased Number of Turns in Work Coil

The challenge to heating aluminum, copper, and any other low-resistivity materials is the low reflected resistance. One straightforward approach is to increase the number of turns in the work coil. As the magnetically-coupled coil/pan is essentially a loosely-coupled transformer, the reflected real resistance at the coil terminals is proportional to the square of the number of turns, neglecting losses in the coil itself. The problem is that the inductance of the coil also increases. The resultant effective coil leakage inductance associated with increased turn count would require impractically high resonant voltages (on the order of kilovolts or tens of kilovolts) to deliver sufficient power at the desired frequency. Proximity and dielectric losses also start to play a role as the coil becomes wound more densely. The resonant voltage, as well as the AC losses can be reduced by operating at lower frequency, but this would require larger resonant and filter components, potentially produce audible noise, and would not allow for utilization of skin effect to further increase pan resistance.

It should also be noted (although not limited to increased turn count), that the high levels of flux interacting with high induced eddy currents can create repulsive Lorentz forces capable of moving or lifting the pan off of the cooker.

B. High-Frequency Skin Effect

At high frequencies, currents tend to crowd toward the surface of conductors due to skin effect. This results in an increased effective resistance of the conductor as frequency increases. By this principle, the effective resistance of a cooking vessel or other metal object can be increased by operating at high frequency and confining induced eddy currents to a thin “skin” on

the surface of the metal. This technique is employed in various industrial processes and is already employed to some degree (in conjunction with other techniques) in current all-metal induction cooker models. Because the effective resistance of the material is increased and therefore the induced currents are lower for a given power level, the use of skin effect also reduces the magnitudes of Lorentz forces acting on the cooking vessel. The maximum usable frequency for induction cooker applications is currently limited by inverter capabilities and also by increased coil and capacitor losses at elevated frequencies [1]. Modern silicon-carbide devices are evaluated for use in extending practical induction cooker switching frequency in [2]. A half-bridge inverter is built using SiC normally-on VJFETs and used to drive a series-load-resonant induction coil/tank. The circuit is successfully operated at 450kHz, however the output power is limited to 120W due to coil and/or resonant capacitor limitations.

A series-resonant induction heating circuit driven by a high-frequency full-bridge inverter using silicon MOSFETs at frequencies as high as 1MHz is experimentally evaluated in Chapter III. Although the reflected resistance of the pan increased significantly at these frequencies, the AC losses in the coil became difficult to mitigate, resulting in poor overall efficiency.

There are methods of operating the induction coil at frequencies higher than the switching frequency of the inverter in order to overcome limitations posed by efficient inverter switching frequency. Various single-switch topologies have been implemented in a large number of low-cost on-the-market induction cookers. A single-ended multi-resonant topology consisting of a series-load-resonant coil/tank driven by a single IGBT and DC bus link inductor has the ability to be operated as a frequency doubler. In the multi-resonant design, the coil can be driven at twice the frequency that the IGBT is actually switched at. The primary tank (coil and series capacitor) is resonant at twice the switching frequency. Partial resonance with the DC link

inductor allows for excitation at half of the resonant frequency. The multi-resonant conditions also all for an operating point to be obtained where the IGBT achieves both zero-voltage turn-on and zero-current turn-off. It is also possible to switch the different resonant capacitors into the circuit to select conventional or double-frequency operation in order to adapt to different cookware materials. There are a few disadvantages to this design. It is highly difficult to vary output power while maintaining soft switching conditions [3]. The switch also experiences high voltage stresses and has no clamping to prevent damage from voltage spikes or other overvoltage conditions.

A time-sharing topology, consisting of two multi-resonant single-switch legs in proposed in [3][4] as a means of reducing switching losses and offering improved control capabilities. The topology, shown in figure 2.9, consists of a series-resonant coil and capacitor that is coupled via secondary resonant capacitors to two legs, each consisting of an IGBT and DC link inductor. The two legs are then driven in an interleaved manner so that excitation of the tank is carried out by the alternating sequence. The circuit presented in [3][4] used a switching frequency of 50kHz and switched resonant capacitors to operate the coil at 100kHz for low-resistivity materials and 50kHz for ferromagnetic metals. The main advantage of this topology over the single-leg, single-ended multi-resonant inverter is that the two legs can be phase-shifted to control output power over a wide range while maintaining soft-switching conditions. The disadvantage is that this topology has a high passive component count over the single-leg design and other proposed topologies. Also, with recent improvements in semiconductor devices, it is now feasible for an IH circuit to have a switching frequency higher than the 100kHz that was achieved by doubler-action.

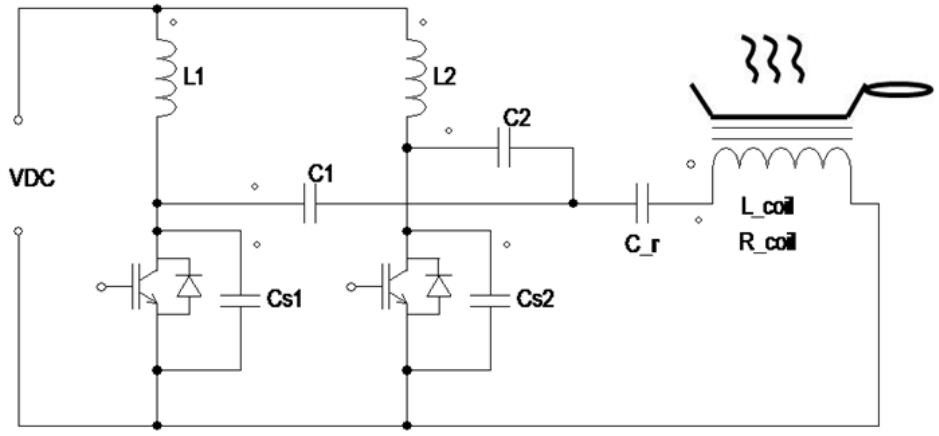

Figure 2.9 Time-Sharing Multi-Resonant Dual-Single-Leg Topology Proposed in [7][8]

A dual-wound coil topology is proposed in [5]. This involves a coil consisting of two parallel windings, each driven by a separate single-ended, single-switch inverter. The two windings are each operated at 20kHz with a phase shift between them. The interleaved drive scheme results in an effective coil frequency of 40kHz applied to the cooking vessel. This allows for the induction load to be driven at twice the switching frequency and therefore reduce inverter losses. This offers limited benefit, as modern semiconductor devices now allow for efficient operation at much higher frequencies without the use of the more-complex topology. Another advantage of this design is potentially increased high-frequency coil efficiency. Each winding only operates at half of the effective frequency, resulting in reduced AC losses and improving coil efficiency at high frequencies. The disadvantage of this design though is that with two windings, each only has half of the available turns-density, therefore reducing the effective amp-turns available from each winding.

C. Harmonic Operation

An alternative method of operating the induction load at frequencies higher than the switching frequency is to use upper harmonics in a voltage-sourced inverter output to excite the resonant tank. In order to drive the work coil at higher frequencies than the inverter is otherwise capable of, the resonant tank can be designed for resonance at an odd harmonic of a voltage-sourced inverter's switching frequency as proposed in [6][7][8][9]. The resonant current is then an odd harmonic of the actual switching frequency as shown in figure 2.10. The waveforms are shown in an ideal in-phase condition for illustration purposes. This harmonic approach is used in some on-the-market models. Most of these designs still only operate the coil in the 100k-200kHz range at the most. Another advantage of this technique is that there is an effective impedance transformation associated with harmonic operation. According to Fourier decomposition, the harmonic content of the inverter's square-wave output is:

Equation 1: Fourier Decomposition of Ideal Square-Wave Inverter Voltage Output

$$V_{inv} = \sum_{n=1,3,5,7,\ldots} \frac{V_{amp}}{n} sin(n * 2\pi * f_{sw})$$

Where V_{amp} is the amplitude of the inverter square-wave output equal to the DC bus voltage (ignoring device voltage drop), f_{sw} is the switching frequency, and n represents the n^{th} harmonic.

Based on this principle, there is an effective n:1 voltage step-down ratio when the tank circuit is resonant at the n^{th} harmonic of the excitation frequency. This is used to allow for matching to the low impedance reflected by an aluminum IH load. Operation at the third harmonic results in an effective voltage step-down of 3:1 or a transformation of load impedance of 1:9. By changing switching frequency and/or switching different resonant capacitors into the circuit, the effective impedance ratio can be selected. Because higher frequency is preferred for

low-resistivity materials, most designs at least switch different resonant capacitors into the circuit. Here, the switching device must handle the high resonant currents and voltages.

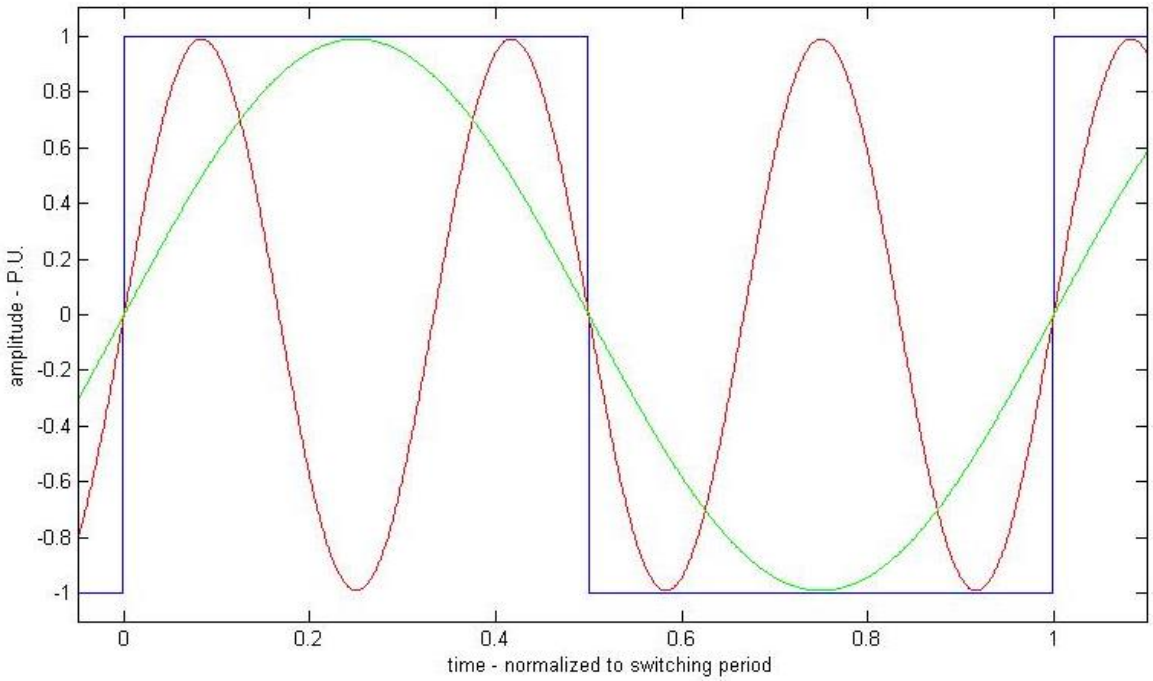

Figure 2.10 Inverter Voltage (blue) and Resonant Current Waveforms for 1st (green) and 3rd (red) Harmonic Operation

The topology presented in [6][7] involves a half-bridge IGBT inverter switched at 23.3kHz used to drive a series-load-resonant tank that is resonant at approximately 70kHz. A relay is used to switch between resonant capacitors to select 23.3kHz first-harmonic operation for ferromagnetic steel/iron cookware or 70kHz third-harmonic operation for low-resistivity metals. In [8][9], a similar resonant topology is presented, only using a boost-half-bridge (B-HB) inverter. The inverter is switched at 20kHz with coil/tank resonance at 20kHz for first-harmonic and 60kHz for third harmonic operation. Relay capacitor switching is also used. The B-HB topology allows for the effective DC bus voltage to be increased above the available rectifier output. This is not necessarily a meaningful advantage in the induction heating of

aluminum, as the main challenge is that the low reflected resistance favors an impractically-low DC bus voltage for use with a series-resonant topology. The B-HB topology does however offer the ability to adjust the effective bus voltage to compensate for variations in reflected resistance from different cookware. Most induction cooker topologies use a natural power-factor correction (PFC) approach due to component count and cost as food heating is not impacted by 120Hz ripple. Instead, the circuit proposed in [8][9] has a filtered DC bus with a front-end power-factor correction rectifier in order to prevent noise and vibration associated with twice-line-frequency modulation of electromagnetic forces acting between the coil and pan.

A disadvantage of the harmonic approach is that the inverter operates at a low power factor and body diode conduction is inherent over a significant portion of the switching cycle. This becomes a more significant drawback as the high circulating power, resonant current, and resonant voltage make efficiency most critical when heating low-resistivity metals.

D. Flux Concentration

One or more devices (such as patent US7049563 B2) [10] for concentrating flux to a small portion of the cooking vessel and therefore increasing the effective resistance have been patented and are used in existing all-metal cooker models. This involves a low-resistivity metal structure, such as shown in figure 2.11, between the coil and cooktop with a geometry that interacts with the alternating magnetic field and focuses the flux on a small portion of the pan. Focusing the flux on a smaller metal surface confines the majority of induced eddy currents to this small region, resulting in increased current density through a given area and improved effective resistance. This design also results in a significant reduction of Lorentz forces acting on the pan. The increased effective resistance results in lower coil current and lower net induced

eddy currents and therefore a lower degree of interaction. It is also theoretically possible that currents induced in the flux-concentrating structure create a flux that interacts with eddy currents in the cooking vessel to create an attractive effect. Although designed to minimize inductive heating of itself, the structure still experiences significant heating and therefore, overall efficiency is impaired if there isn't a low-thermal-impedance path from the structure to the pan. Here, the cooking vessel is heated by both induction and thermal transfer from the heated metal piece below the cooktop. Although patents exist, no additional published works have been found on this technique.

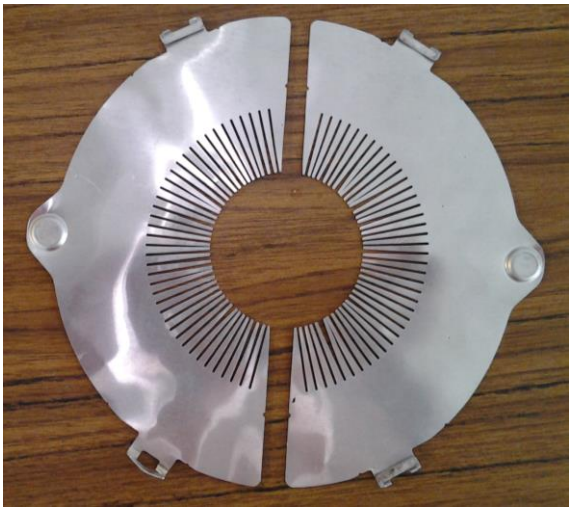

Figure 2.11 Main Element of Flux-Concentration Device as Removed from an Existing Induction Cooker

E. Parallel-Resonant and L-C Impedance Matching

In a parallel-resonant topology, the inverter does not carry the entire resonant current. Operating the circuit near resonance allows for the coil resistance to be transformed to a much higher terminal value. However, the coil voltage is presented to the inverter output. A voltage-sourced inverter (full- or half-bridge) is not favorable here for multiple reasons. The coil voltage encountered when heating a low-resistivity material (on the order of kilovolts) requires an

impractical DC bus voltage or a boost stage before the main inverter stage. Additional matching is required to provide a suitable impedance to the inverter without a significant reactive component. The parallel-resonant capacitor is connected across the inverter, which will subject the switches to severe stresses if not turn-on doesn't occur at zero-voltage conditions. The high capacitance would also make these conditions more difficult to achieve.

The parallel-resonant coil/tank circuit can be directly driven using a current-sourced topology, where output voltage is not clamped to the DC bus voltage. Various single-switch topologies are already employed in several on-the-market induction cooking devices for ferromagnetic cookware. The disadvantage of this topology is that the switch must still block the entire voltage and that there is no inherent voltage clamping to protect the switch(es) from overvoltage. The voltage requirements for the switches become a problem with the high resonant voltages encountered when the coil is coupled to a low-resistivity induction load. Here, devices with sufficient blocking capability would have significant conduction loss under the required output current.

The parallel-resonant topology can also be driven with a voltage-sourced inverter by means of a matching network. Figure 2.12 shows an inductively-matched, parallel-resonant topology that can be used to match the coil to a resistance suitable for inverter operation as well as providing a resistive or slightly inductive load to support efficient inverter operation. The main disadvantage to this design is that its matching characteristics are frequency dependent. As a result, performance is significantly impacted when frequency and coil inductance are changed with the use of cooking vessels of different sizes and materials. The use of variable capacitors and inductors is assumed to be not practical or affordable for stovetop cooking applications.

This particular design would also require a means of DC blocking or control on the inverter output.

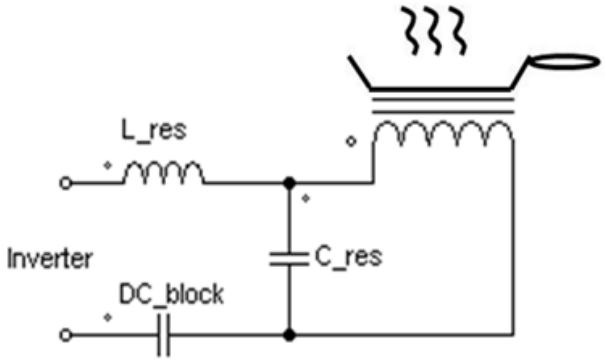

Figure 2.12 Inductor-Matched Parallel-Resonant IH Topology

F. Impedance Matching via Transformer

Transformer-matched induction heating devices are used in a variety of industrial and laboratory applications over a wide range of power levels, however the use of a matching transformer is generally avoided in induction cooking devices due to size and cost. For heating ferromagnetic cookware, a coil can be easily designed to reflect a suitable impedance for the rest of the circuit and a transformer is not necessary. In existing induction cooker technologies, the work coil has been designed to meet the electrical constraints of the inverter and resonant tank. This becomes an obstacle to the heating of low-resistivity materials in that efficiency of the coil becomes much more critical in these applications. Here, the use of transformer-matching is beneficial in that it allows for additional freedom in the design of the coil with less constraint from other circuit requirements. Aside from size and cost, the only disadvantage is that it doesn't allow for the matching ratio to be adjusted by means of frequency as can be done with L-C matching networks and harmonic-based techniques.

Figures 2.13 and 2.14 show two different transformer-matched induction heating topologies. In fig. 2.13, the matching transformer is part of the resonant tank. Here, the resonant capacitors do not have to handle the high coil current and the transformer operates with sinusoidal voltages. There are two problems with this design though: capacitor voltage rating and transformer size. The voltage across the coil in the resonant tank circuit can be on the order of kilovolts. The voltage reflected through the transformer. The voltage reflected to the primary of the step-down transformer would be much larger and therefore result in impractical voltage requirements on the resonant capacitors. Because the transformer is in the resonant tank, it must handle all of the circulating power, greatly increasing the size and cost of the transformer as well as associated losses. When coupled to a low-resistivity load, the lower reflected resistance results in an impedance that is dominantly inductive with a small resistive component. This results in a resonant circulating power that can be more than an order of magnitude larger than the real power delivered by the circuit.

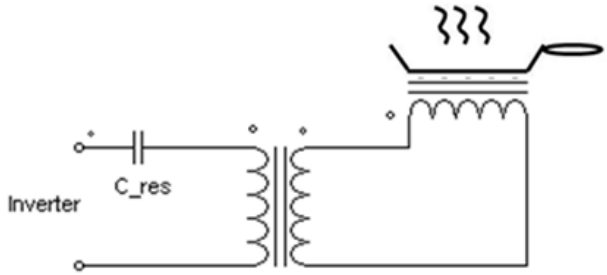

Figure 2.13 Transformer Inside IH Resonant Tank

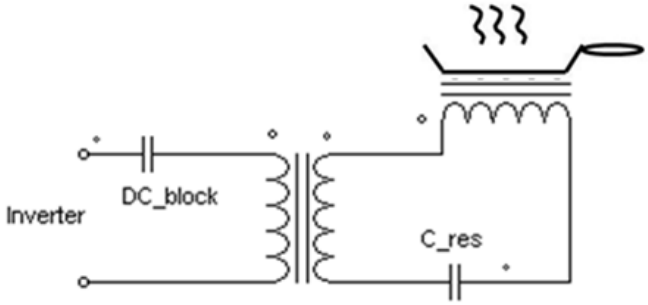

Figure 2.14 Transformer Driving Series-Load-Resonant IH Circuit

The proposed design will focus on the topology in in fig. 2.14, where the matching transformer is used to couple the inverter to a conventional series-load-resonant circuit. Here, the transformer is only required to carry the real power delivered to the tank, with the exception of the reactive power involved when not operating at resonance. One disadvantage to this design is that the transformer is operating with the harmonic content of the square-wave inverter output voltage. The other issue is that the transformer parasitics play a role in the current waveform seen at the inverter and need to be designed accordingly. This is not necessarily a disadvantage though, in that the transformer can be designed to provide soft-switching conditions for the inverter (similar to LLC converter design approach) at an operating point where the LC tank would not provide such. The inverter can be operated at the resonance of the coil and capacitors, which would result in a purely resistive terminal impedance at the secondary. The magnetizing inductance of the transformer can then be designed to provide an inductive load to the inverter suitable for zero-voltage switching conditions. An additional consideration with this topology is the need for a DC blocking capacitor on the transformer primary if a half-bridge inverter or a full-bridge inverter without a means of DC current control is used.

III. EVALUATION OF HIGH-FREQUENCY OPERATION TO UTILIZE SKIN EFFECT

Operating an induction cooker at high frequencies results in skin effect in the eddy currents induced in the cooking vessel, increasing the effective resistance. This is employed to some degree and in conjunction with other techniques in current all-metal induction cookers and in some models compatible with non-ferromagnetic stainless steel cookware. In current technologies, the operation frequency is limited to 100k-200kHz due to inverter switching efficiency and losses in resonant elements. In order to evaluate the feasibility of further increasing operating frequency to further utilize skin effect to increase the reflected resistance of aluminum cookware, an experimental high-frequency circuit was built and tested at 950kHz.

Design and Construction of Experimental Circuit

A conventional series-load-resonant topology (figure 3.1) consisting of the work coil and series-connected resonant capacitors was operated at 950kHz. A full-bridge inverter was built using BSC027N08NS5 (80V, 2.7mΩ) silicon MOSFETs from Infineon Semiconductor as shown in figure 3.2. As indicated by the 80V rating, the inverter was designed for low-voltage, high-current operation as the reflected resistance is still expected to be low. The low threshold voltage of the devices allowed for gate drive voltage to be reduced to 9 volts without compromising conduction performance in order to reduce gate drive losses. The Super SO-8 package was chosen for its low parasitic inductances and high-frequency suitability. Extreme care was taken in the PCB layout to reduce parasitics. One limitation is that the SO-8 device packages do not provide for high cooling performance. Thermal vias were used near the switches to provide heat

transfer to heatsinking on the back of the PCB. Isolated gate drivers (Si8234) with boost-strap supplies were used on all four switches. Potentiometers were used to vary the analog on-chip dead-time. Heatsinks were mounted to the case of the gate drivers, as driver dissipation at 1MHz with the 9-volt boost-strap supply approached the datasheet limit of the chips. High-frequency 10µF bus capacitors were placed as close to each switch leg as possible. Additional film capacitors (not shown in figure 3.2) were later added to also allow for operation at lower frequencies.

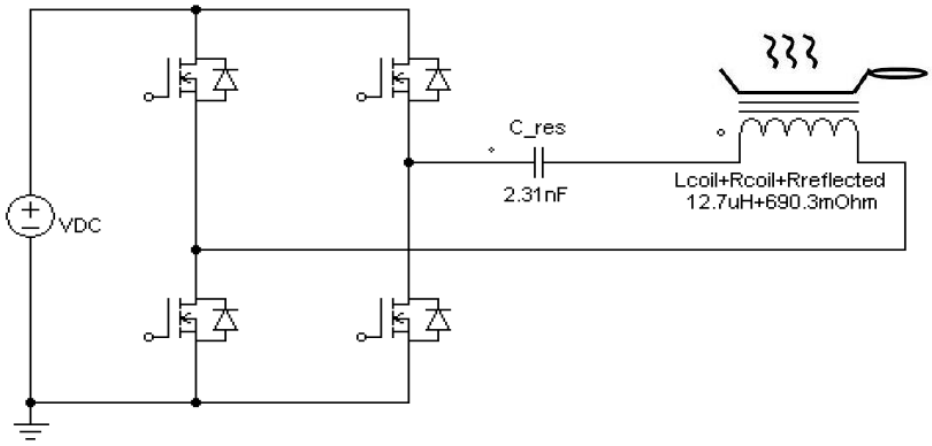

Figure 3.1 Basic Schematic of Experimental High-Frequency Series-Resonant Circuit

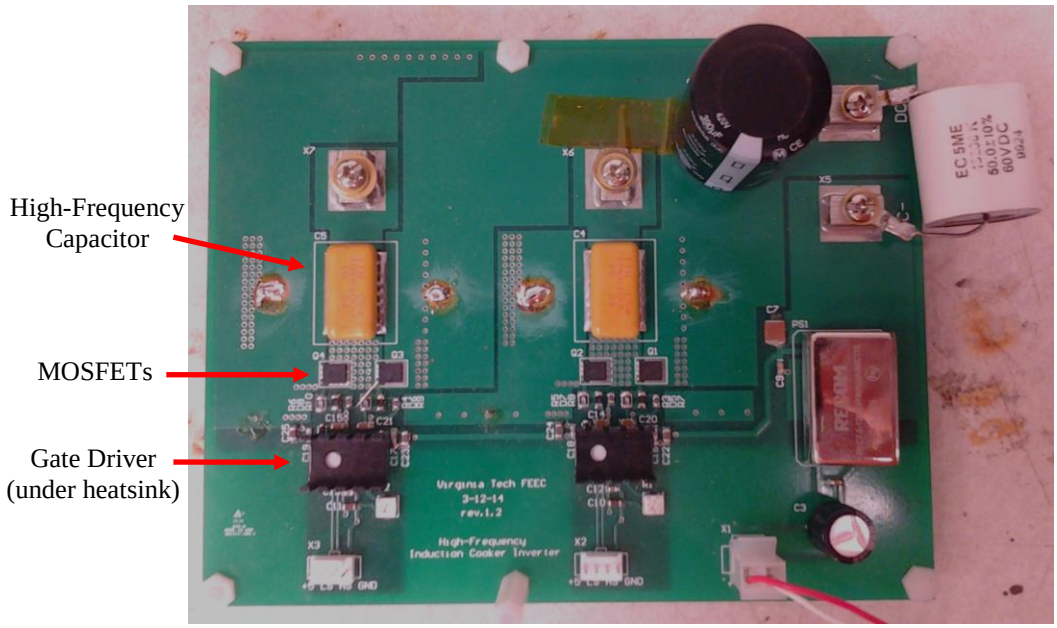

Figure 3.2 High-Frequency Full-Bridge MOSFET Inverter

For this application, the work coil was specifically designed to reduce AC losses at high frequencies. A low number of turns was chosen to reduce proximity losses and dielectric heating losses even though the low turns-count requires higher resonant current to deliver a given amount of power. The coil consisted of 19 turns of #9AWG-equivalent, #46AWG-stranded type-2 Litz wire with a high-temperature PTFE outer jacket. The coil was mounted with a 0.7mm spacing between windings (figure 3.3a) in order to reduce dielectric heating between adjacent windings. An array of 16 ferrite bars (figure 3.3b) was mounted under the coil to reduce stray flux and improve coupling to the pan.

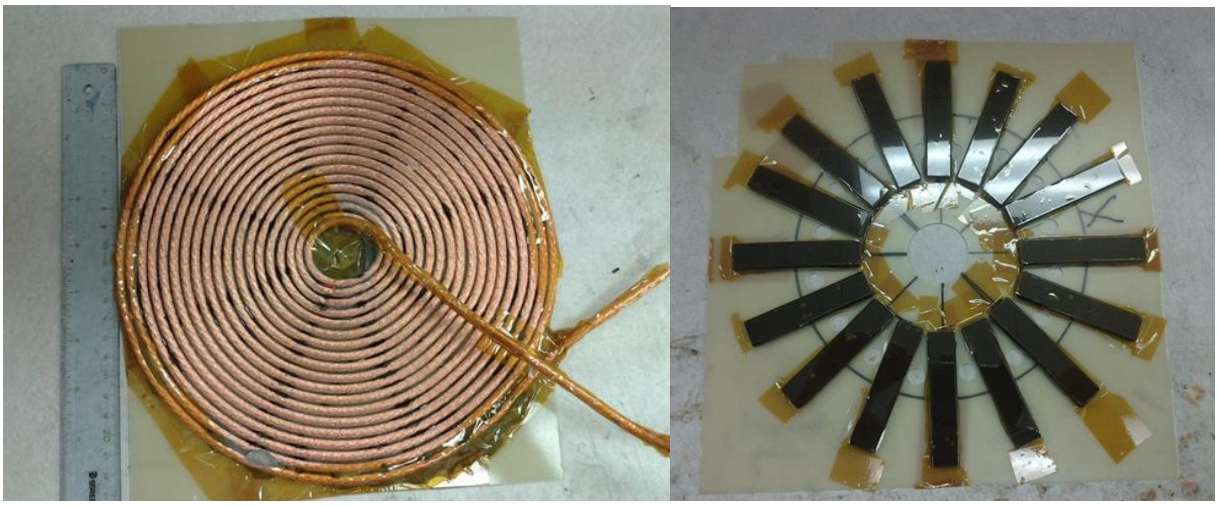

Figure 3.3 (a) 19-Turn, 0.7mm-Spaced Planar Coil (left) and (b) Ferrite Bar Array (right)

When an aluminum pan (24cm bottom diameter) was placed on the coil and ferrite assembly, the equivalent inductance of the coil terminal inductance was 12.7µH @ 200kHz. The challenge with this design was in achieving a suitable resonant frequency while using resonant capacitors capable of handling resonant currents in excess of 20 Amperes. A series-resonant capacitance of 2.31nF resulted in a resonant frequency of 930kHz. This capacitance consisted of a 3-parallel, 13-series combination of 10nF, 230VAC high-current polypropylene capacitors (5PT46J103K from Electronic Concepts Inc.). Individually, they are rated at $10A_{rms}$ at 25˚C. The series combination was divided with 6 on one end of the coil and 7 on the other in order to reduce common-mode voltage on the coil. Figure 3.4 shows the circuit as built and tested.

It was discovered in previous experimentation that the capacitive impedance between the coil and pan is low enough at 1MHz to couple potentially hazardous common-mode voltage and current to the pan. The capacitance between coil and pan was measured to be 93pF which is an impedance of -j1711Ω @ 1MHz. With the observed coil voltage of $1.73kV_{rms}$ as an example, the common-mode coil voltage would be approximately $865V_{rms}$ with all of the capacitors on one leg of the coil and assuming inverter output to be insignificant relative to resonant voltage. The

effective voltage delivered to the pan would then be 865V through a Thevenin impedance of 1.7kΩ, which would pose a potential hazard. With the resonant capacitors evenly divided between both legs of the coil, the theoretical common-mode voltage coupled to the pan is zero. The actual value is finite (although significantly lower than previous case) as the inductive "midpoint" of the coil is different from the "center" of the capacitively-coupled surface since an outer turn involves more wire than an inner turn. This technique still has one limitation in that if a pan of smaller diameter than the coil was used, the actual common-mode voltage coupled to the pan would not be cancelled and a shock and/or RF burn hazard would persist.

The circuit was operated with a switching frequency higher than resonance by a large enough degree that the resonant current was able to discharge device capacitances and provide zero-voltage turn-on of the MOSFETs. Frequency was adjusted to maintain these conditions while minimizing body-diode conduction, as the device packaging made power dissipation critical.

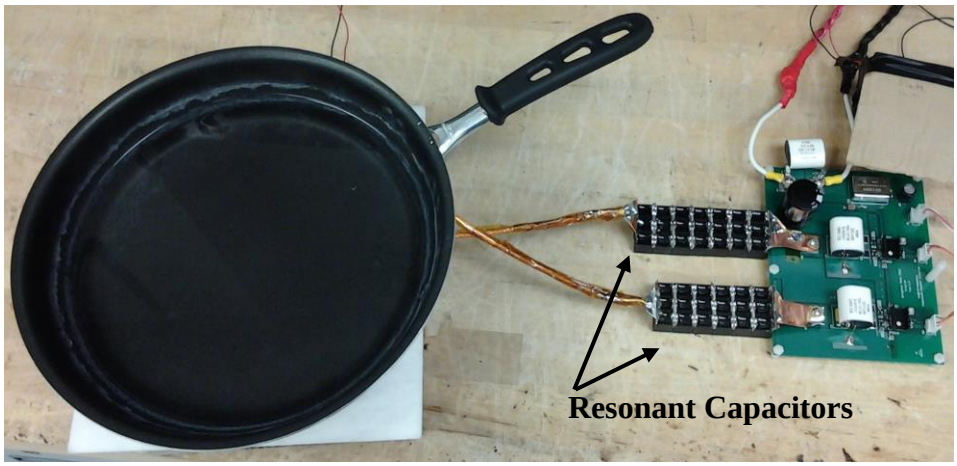

Figure 3.4 Experimental High-Frequency Induction Cooker Circuit

Experimental Results

An inverter output power of 343W was achieved when operating the circuit at 948kHz. The limiting factor on output power was the temperature of the MOSFETs and the temperature of the coil. The low-stray-inductance Super SO-8 package of the devices offers limited thermal transfer capabilities and does not allow for suitable cooling for higher output power under these operating conditions. At this power level, the resonant current was $21.1A_{rms}$, corresponding to an effective reflected coil resistance of 770mΩ. The coil voltage was $1.73kV_{rms}$. The 343W output power was achieved with an input current of 19.1A @ 20.3VDC, resulting in an inverter efficiency of 88.5%. An additional 3.4W was consumed by gate drive, measured at input to the isolated DC/DC converter providing the 9-volt boost-strap supply.

After 5 minutes of operation at this power level, the coil reached a temperature of approximately 95˚C. Although the Litz wire was rated for operation at 200˚C, the epoxy used to support the 0.7mm spaced coil had much lower temperature handling. The measured output power was measured as the power supplied to the resonant tank by the inverter. This consists of the power delivered to the cooking vessel along with losses in the coil and resonant capacitors. An analytical measurement of coil efficiency was performed by separating coil losses from the total reflected resistance at the frequency of interest. The AC resistance of the coil when not in close proximity to any conductive or ferrous objects was found to be 359mΩ at 948kHz based on a polynomial approximation applied to a series of measurements. This procedure is presented in Chapter IV. Assuming the coil AC resistance to be constant as a component in the total 770mΩ observed terminal resistance, the coil efficiency is 53.4%.

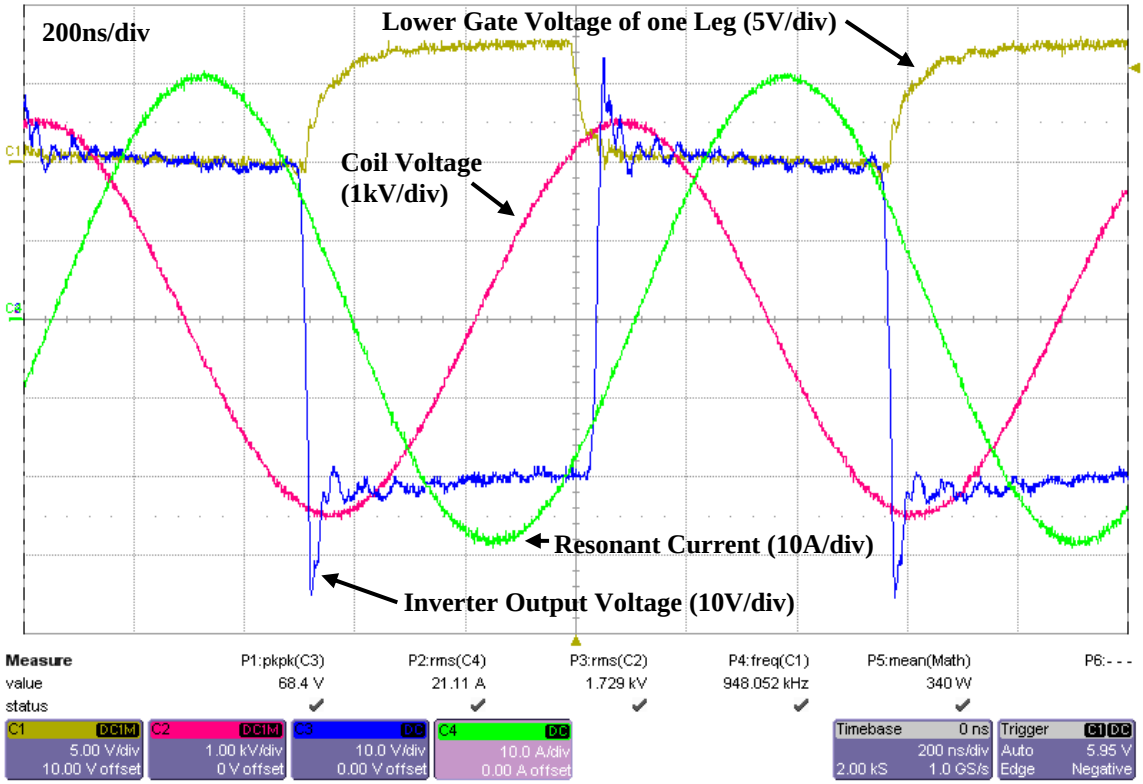

Figure 3.5 High-Frequency IH Inverter Operating at 948kHz with 343W Output
All 200ns/div.

The inverter is achieving zero-voltage turn-on of the switches, resulting in the clean gate signal shown in figure 3.5. There is significant overshoot in the inverter output voltage, caused by parasitic inductances and the high dv/dt experienced at switch turn-off. As shown in figure 3.5, the resonant current is lagging behind the output voltage by a much larger interval than is required to charge device capacitances (voltage transition of inverter output (blue trace)). A higher power factor could not be achieved, as this interval was required to fully turn on the latter device before commutation of current conduction. In order to compensate for the gate-charging time, turn-on delay, and rise-time of the devices and allow for improved power factor, gate turn-

on would have to be initiated before turn-off of the complimentary device, which was not possible with the means of control used in this experiment.

The losses in the inverter power stage consist of turn-off losses, forward conduction, and diode conduction. Turn-on losses are essentially zero due to the zero-voltage turn-on. The phase shift between current and inverter output voltage results in significant diode conduction losses. Although operation was not sustained due to potentially destructive amounts of overshoot and ringing from loss of zero-voltage turn-on, it was determined by thermal measurement that efficiency was actually improved by operating with current and voltage in phase and no diode conduction.

IV. INDUCTION COIL DESIGN AND EFFICIENCY

The low reflected resistance and high coil current make coil efficiency critical to the functionality of the aluminum induction cooker. The efficiency of the work coil pertains to the portion of real resistance seen at the terminals reflected from the cooking vessel versus the portion of resistance due to coil losses. Both of these factors are frequency-dependent. As frequency is increased, the effective resistance of the cooking vessel increases due to skin effect. But the AC losses in the coil also increase. Due to these relationships, there is an optimum frequency for a given coil design at which efficiency is maximized. Further increasing frequency results in an increase in the percentage of power dissipated in coil losses. Further decreasing frequency results in a decrease in effective vessel resistance, requiring higher coil current and increasing coil losses. A few different experimental coil configurations were built and their efficiencies were measured as a function of frequency in order to select the best coil design and the optimal operating frequency to maximize its efficiency.

Induction Coil Efficiency Measurement Procedure

For circuit design purposes, the coil impedance of the pan-coupled coil was modeled as a series combination of reflected pan resistance, coil resistance, and leakage inductance (figure 4.1a) which can be simplified to a terminal impedance of a single resistance in series with leakage inductance. A more accurate model (figure 4.1b) includes the magnetizing inductance in parallel with the previous impedance. A model that is accurate at higher frequencies would also include parasitic inter-winding capacitances.

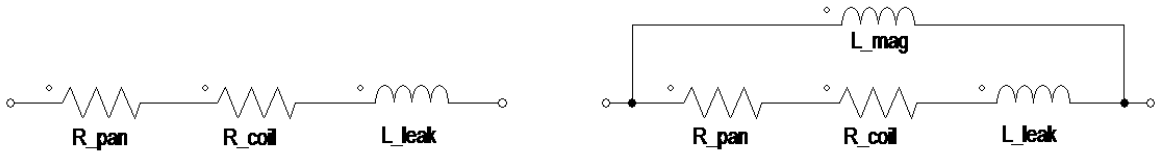

Figure 4.1 Modeling of Coupled IH Coil (a/left) simplified, (b/right) Including Magnetizing Inductance

An accurate direct resistance measurement of an aluminum-coupled or non-coupled coil is not possible as the magnitude of the real impedance component is significantly smaller than the reactive component. Instead, a low-ESR, low-dissipation polypropylene film capacitor or combination of capacitors was connected in series with the coil to produce resonance at a frequency of interest. A frequency response analyzer was then used to measure the real resistance of the circuit at resonance. This resistance consists of both the resistive component of the coil impedance and the ESR of the capacitors. This procedure was repeated using different values of capacitors to measure resistance at difference frequencies. The data was then assigned a 2^{nd}-order polynomial approximation using Matlab in order to obtain a frequency versus resistance function.

Measurement of coil efficiency involved measuring the total resistance reflected to the coil terminals when coupled to an aluminum pan and measuring the losses in the coil as resistance of the coil when not in close proximity to conductive or ferrous objects. The AC resistance of the coil itself with no conductive objects in close proximity was measured over a wide frequency range. The coil was not mounted on the ferrite sheet for this measurement as the increased inductance made it impractical to achieve resonant frequencies in the range of interest using capacitance values available for low-ESR polypropylene capacitors. An aluminum pan was then placed on the coil/ferrite assembly and the total reflected resistance was then measured over a frequency range. From these two sets of data, the frequency-efficiency relationship was calculated from the 2^{nd}-order polynomial equations for the two measurements. From the resulting

equation, the most efficient coil (within constraints of practical current, voltage, and frequency limits) was determined along with its optimal operating frequency.

Coil Designs and Measured Efficiency Data

This above procedure was performed for three different experimental coil designs. All three designs use heavier-gauge wire and therefore lower turns-density than is used in conventional on-the-market induction cooker technologies. A higher number of turns is conventionally preferred in order to increase the reflected resistance presented at the coil terminals, however there are two reasons for the converse. The low number of turns was chosen to reduce the coil inductance and therefore reduce the resonant voltage in order to keep it within practical resonant capacitor constraints and safety considerations. Reducing the number of turns also potentially reduces the AC losses of the coil, allowing for more efficient operation at high frequencies. When coupled to the aluminum pan, all three coils were placed on a ferrite sheet as was used in the functional induction cooker design. The ferrite sheet consisted of an array of E-30 size transformer E-cores (3F3 material by Ferroxcube, Inc.) placed with the flat back edge upward (shown in figure 4.2). The 9x37 array of cores had dimensions of 26x27cm. The pieces in the center were removed to allow wire routing under the sheet.

Figure 4.2 Ferrite Sheet Consisting of 9x37 Array of E-30 Size E-Cores

22-Turn Single-Layer Coil (figure 4.3a):

22 Turns of #9AWG-equivalent, #46AWG-stranded Litz wire tightly wound to maximize turns-count for a single-layer coil.

19-Turn Single-Layer Coil with 0.7mm Spacing Between Turns (figure 4.3b):

19 Turns of #9AWG-equivalent, #46AWG-stranded Litz wire mounted on FR4 board with 0.7mm spacing between turns. The spacing between turns was intended to reduce proximity losses and dielectric heating and therefore allow of more efficient high-frequency operation. A 3D-printed former with circular tracks was used to space the wire. The coil was then epoxied to the FR4 board and the former was removed.

34-Turn Two-Layer Interleaved Coil (figure 4.3c):

34 Turns of #9AWG-equivalent, #46AWG-stranded Litz wire wound in a two-layer coil in order to increase the number of turns for a given diameter and therefore increase reflected resistance. The coil was wound with an interleaved pattern, alternating sides while winding from inside to outside. This was done to reduce losses associated with high voltages between adjacent turns.

The use of two stacked, series-connected single-layer coils would result in higher voltage between top and bottom turns and therefore higher insulation requirements and dielectric losses.

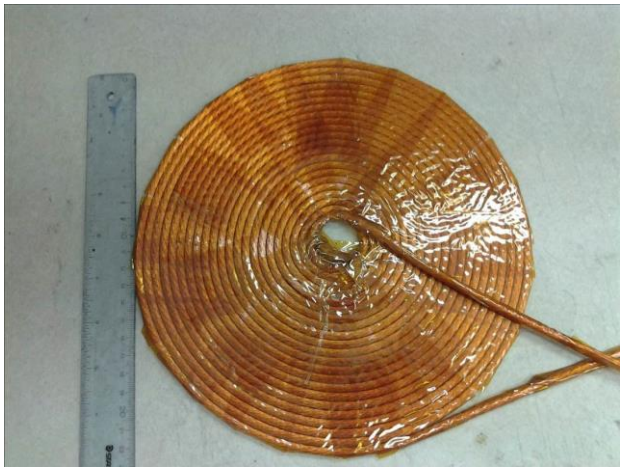

(A) 22-Turn Single-Layer Coil

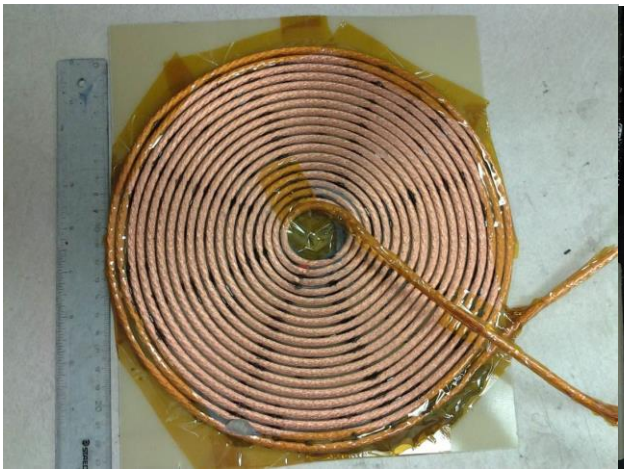

(B) 19-Turn Coil with 0.7mm Turn Spacing

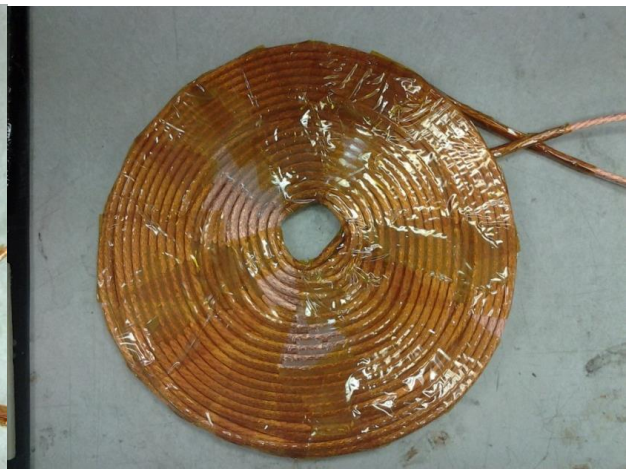

(C) 34-Turn 2-Layer Interleaved Coil

Figure 4.3 Experimental Induction Coil Designs

Parameters of the experimental coils are shown in Table 1. The DC resistance of each of the coils was measured by passing a DC current of 40 Amperes through the coil using a constant-current power supply and then measuring the voltage across the coil. The voltage test leads were connected to the coil termination near the where it was bolted to the power supply leads so as to include termination resistance but not include the impedance of the interface with the power

supply lead in the measurement. All measurements were made when the coil was at 40˚-45˚C. The self-resonance was measured using a frequency response analyzer. The coupled equivalent inductance was measured at 100kHz via using an LCR meter. For this measurement, the coil was mounted on a ferrite sheet with a piece of thin fiber insulation and high-temperature Schott glass placed over the coil and an aluminum pan (24cm diameter bottom surface) placed on the assembly.

Table 1: Parameters of Experimental Induction Work Coils

	19-Turn Single Layer 0.7mm-Spaced	22-Turn Single Layer	34-Turn Two Layer Interleaved
Outer Diameter	238mm	234mm	235mm
Inner Diameter	29mm	28mm	34mm
DC Resistance	24.6mΩ	26.9mΩ	46.5mΩ
Self Resonance	2.5MHz	2.2MHz	1.1MHz
Coupled Equivalent. Inductance @ 100kHz	15.3µH	22.9µH	70.9µH

The measurements of resistance reflected to the terminals of the resonant tank, as well as the resistance presented by coil losses only are shown as a function of frequency in figure 4.4 for the three coils. Both of these values increase with frequency for all three coils. It should be noted that the measured resistances also include the ESR of the resonant capacitors and therefore the measured loss-associated resistance of the coil is comprised of coil resistance, termination resistance, and capacitor ESR. The 34-turn coil exhibits significantly higher reflected resistance from the pan, but also has a much higher self-resistance.

The measured resistances shown in figure 4.4 were then used to derive a function of coil efficiency (equation 2) as plotted in figure 4.5. According to this relationship, the 22-turn coil reaches a peak efficiency of 86.9% at 140kHz and the 19-turn coil reaches a peak efficiency of

84.1% at 146kHz. The small variation in peak-efficiency points indicates that for a planar coil at this frequency, dielectric heating and the portion of proximity losses associated with adjacent conductors do not have a large contribution to coil losses. Although more efficient, the 34-turn coil reaches its peak efficiency of 88.1% at a much lower frequency of 51.5kHz and exhibits a more rapid roll-off of efficiency as frequency is increased. This is likely due to higher dielectric and proximity losses since each turn has a higher number of adjacent conductors (only two with single-layer coil) as well as reduced coil-to-pan coupling efficiency of the multi-layer design. All three coils experience a severe reduction in efficiency as frequency is further increased. The reduced losses of the 0.7mm-spaced 19-turn coil begin to yield a benefit over the 22-turn coil around 700kHz but no advantage is obtained over the frequency range plotted. Although the spaced coil becomes more efficient than the others, efficiency is still poor at this frequency.

Equation 2: Coil Efficiency Based on Resistance Measurements

$$Eff = \frac{P_{pan}}{P_{total}} = \frac{R_{pan}}{R_{total}} = \frac{R_{total} - R_{coil}}{R_{total}}$$

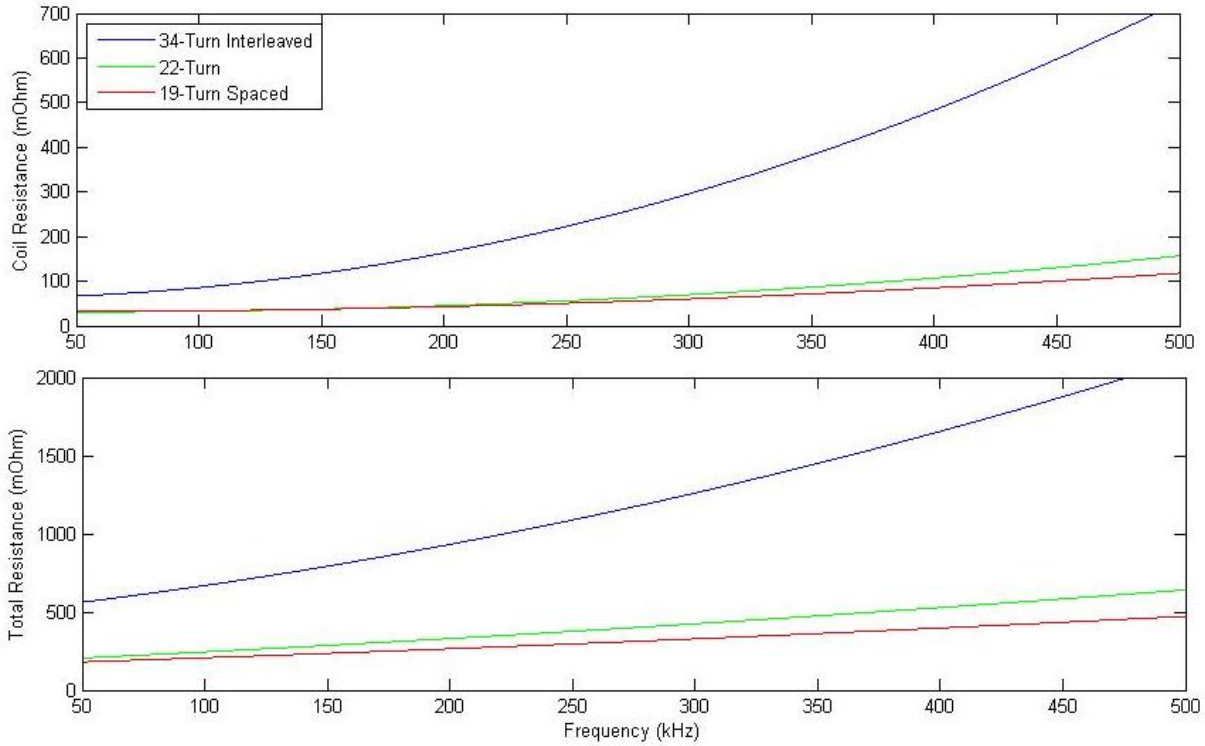

Figure 4.4 Effective AC Resistance of Coil (top) and Total Reflected Resistance with Coil Coupled to Aluminum Pan (bottom) as a Function of Frequency
for 22-turn coil (green), 19-turn, 0.7mm-spaced coil (red), and 34-turn 2-layer coil (blue)

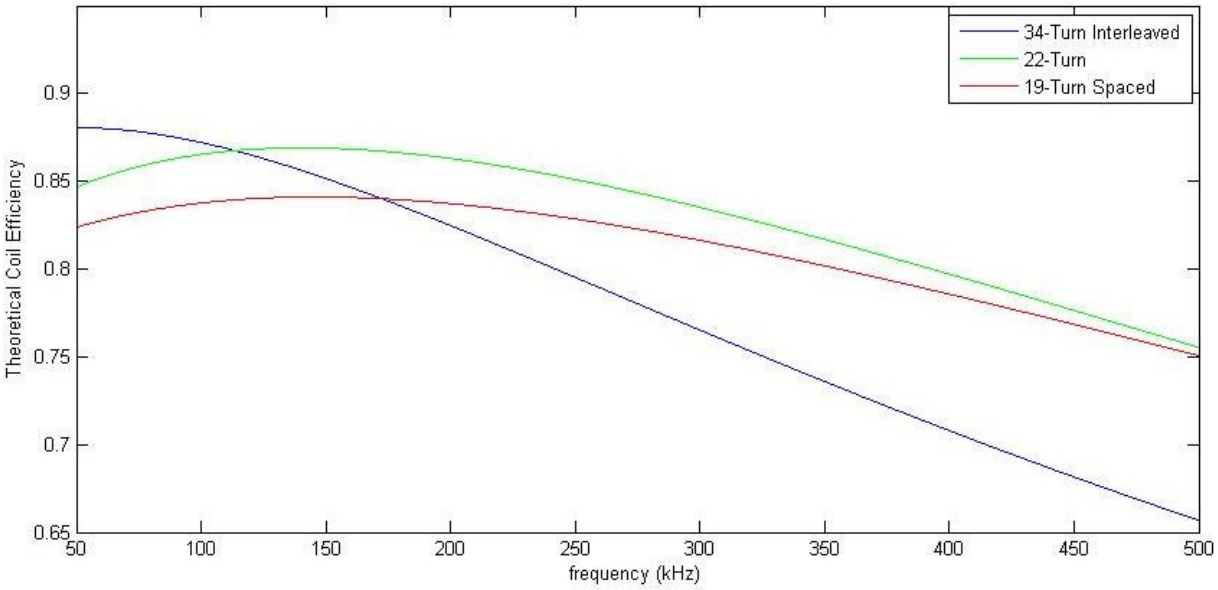

Figure 4.5 Induction Coil Efficiency versus Frequency Based on Resistance Measurements

The calculated coil efficiency was then used to calculate the amount of power dissipated in the cooking vessel and in the induction coil when 1kW is supplied by the inverter as shown in figure 4.6.

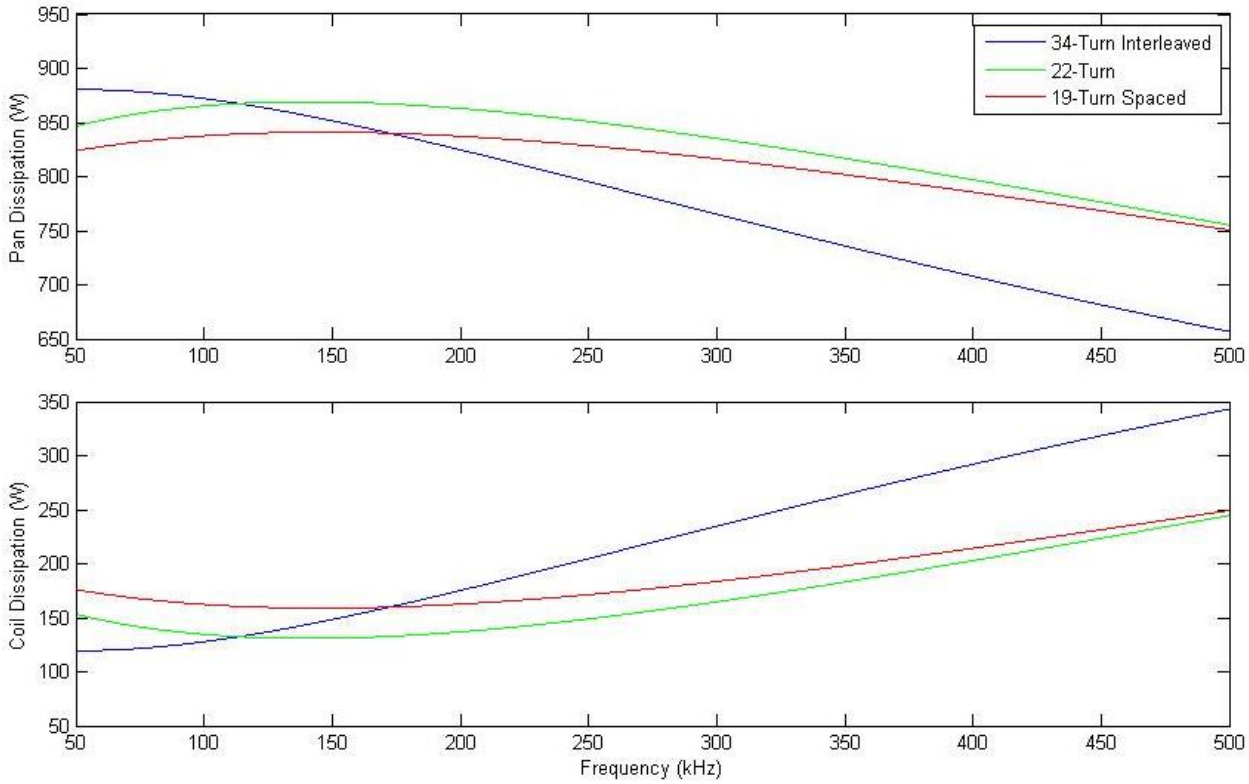

Figure 4.6 Power Dissipated in Aluminum Pan (top) and Power Dissipated in Coil (bottom) versus Frequency for 1kW Supplied to Resonant Tank by Inverter

In order to evaluate the current-handling requirements of the resonant capacitors and other circuit elements, the coil current for 1kW operation (figure 4.7) was determined based on reflected resistance. As expected, the required current is inversely proportional to the number of turns at low frequency and follows the same trend with some deviation as frequency is increased.

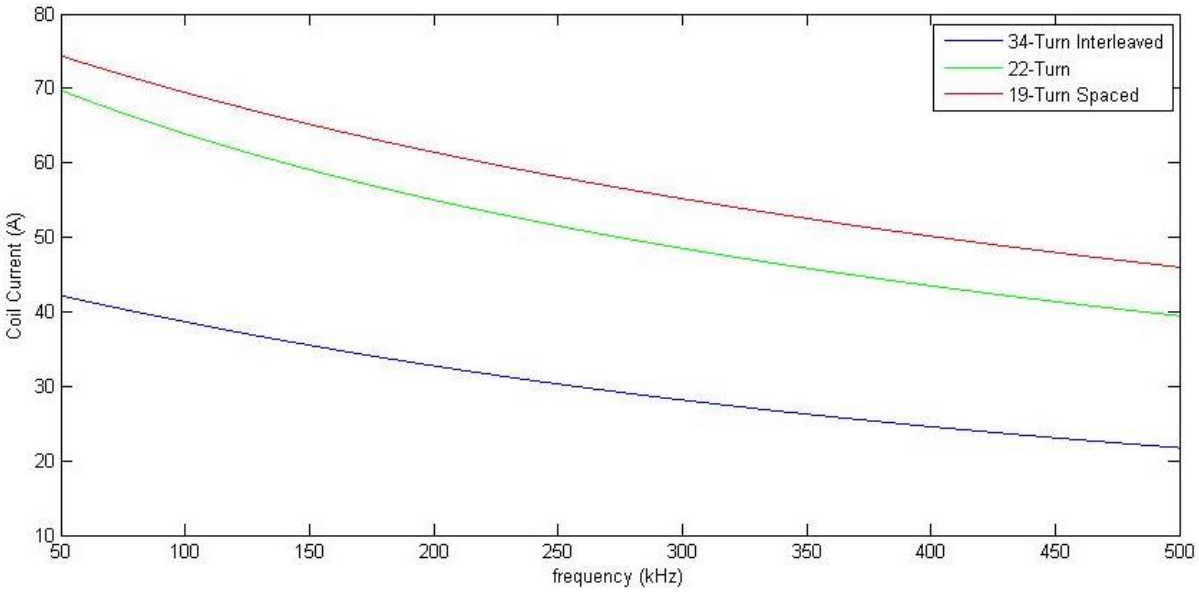

Figure 4.7 Required Coil Current versus Frequency to Deliver 1kW at Coil Terminals

The most efficient design based on the coil efficiency measurement was the 34-turn two-layer coil operating at 51.5kHz. Although not as efficient, the design used in the following work is the 22-turn single-layer coil with peak efficiency at 140kHz. There are two advantages of this design over the higher efficiency 34-turn coil. In order to reduce Lorentz forces acting between the coil and pan, it is preferable to operate the circuit at the highest frequency possible so that skin effect causes the effective resistance of the pan to increase. Also, excess heat can be more effectively removed from the single-layer coil than from the double-layer design.

V. EXPERIMENTAL TRANSFORMER-COUPLED IH CIRCUIT

Design and Construction of Experimental Circuit

The proposed transformer-matched induction cooker topology consists of a work coil with ferrite shielding, series-resonant capacitors, a matching transformer, and a full-bridge MOSFET inverter. The topology is shown in figure 5.1 and the equivalent circuit model (with coil magnetizing inductance lumped into a single coil inductance) seen by the inverter is shown in figure 5.2.

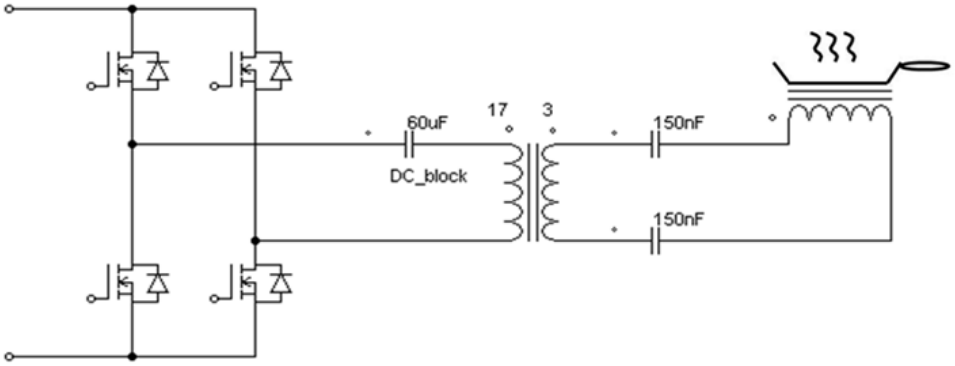

Figure 5.1 Schematic of Experimental Transformer-Coupled IH Circuit

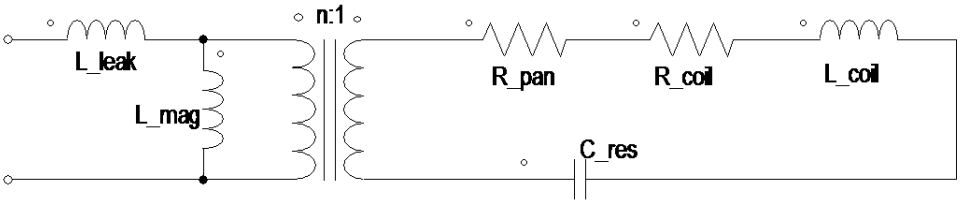

Figure 5.2 Electrical Model of Transformer-Coupled Circuit Seen at Inverter Output

Work Coil:

The work coil is a single-layer planar coil consisting of 22 turns of #9AWG-equivalent, #46AWG-stranded type-2 Litz wire with a PTFE outer sheathing rated for 200ºC. Although higher resonant current is required, the low number of turns in the work coil was used in order to

keep the resonant voltage within practical capacitor and safety limits. This does increase the current stress on the coil and resonant capacitors, but the matching transformer allows for the circuit to be easily driven by the inverter. The low number of turns in the coil also reduces AC losses in the coil at high frequencies, allowing for better utilization of skin effect to increase the effective resistance of the cooking vessel. The coil has an outer diameter of 23cm and inner diameter of 3cm.

The self-resonance of the coil was measured to be near 2.5MHz using a frequency response analyzer (FRA) and the DC resistance was measured to be 26.5mΩ @ 40ºC including the terminations. In order to shield the underside of the coil and to improve magnetic coupling to the cooking vessel, the coil was mounted on a ferrite sheet comprised of small E-30 size E-cores (3F3 material by Ferroxcube, Inc.) turned with the outer flat edge facing upwards, shown in figure 5.3. The same type of cores were placed on their sides around the perimeter of the coil to further improve coupling and to provide a small air gap above the coil for forced-air cooling. With a large aluminum pan (24cm diameter on bottom surface) above the coil, the equivalent inductance was measured to be 22.9uH @ 100kHz using an LCR meter.

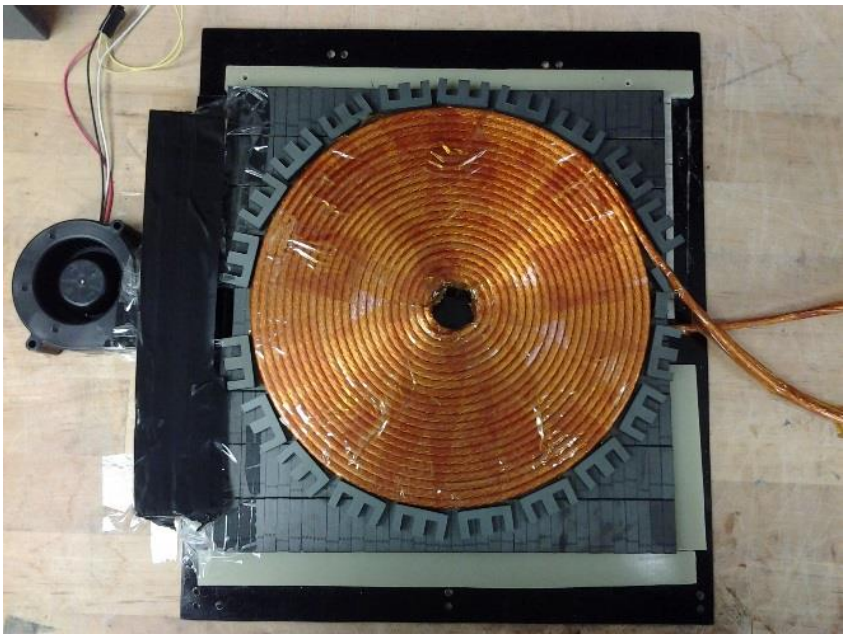

Figure 5.3. 22-Turn Induction Coil Mounted on Tiled E-Core Ferrite Sheet (cooling blower on left)

Resonant Tank:

With the effective coil inductance of 22.9µH, a resonant frequency of 120kHz was achieved using a resonant capacitance of 75nF. In order to deliver 1kW into the 290mΩ, a resonant current of 58.7A_{rms} is required. The resonant capacitor voltage would then be 1.04kV. An output power of 1.5kW (50% above initial design power) would require a resonant current of 71.9A_{rms}. The expected voltage on the capacitors is then 1.27kV_{rms}. In order to handle the required resonant current and voltage, a 4-series, 3-parallel combination 100nF, 460VAC high-current polypropylene film capacitors (5PT46N104K from Electronic Concepts, Inc.) was used. These capacitors have an individual current rating of 37.6A_{rms} @ 100kHz and 25ºC. The series combination was split between the two ends of the coil in order to reduce the common-mode voltage on the coil, therefore reducing the voltage capacitively coupled to the cooking vessel from the coil.

The low reflected resistance of the aluminum-coupled coil results in a high-Q characteristic that is not observed in IH applications involving ferromagnetic materials. At 120kHz, the 22.9µH effective inductance of the work coil results in an impedance of j17.3Ω, which is almost two orders of magnitude larger than the 290mΩ real terminal resistance. A quality factor (Q-factor) can be defined for the resonant tank as:

Equation 3: Q-Factor of Resonant Circuit Based on Energy Storage

$$Q(\omega) = \omega * \frac{max.stored\ energy}{power\ loss}$$

Assuming coil voltage to be exactly 90˚ out of phase with coil current, the energy stored in the capacitors is zero at the instance of peak energy stored in the coil inductance and vice-versa. Here, the peak stored energy stored in the resonant capacitors or coil inductance at 1kW operation is 0.08J as defined by:

$$E_C = \frac{1}{2} * 75nF * \left(1.04kV * \sqrt{2}\right)^2 = 0.08J$$

$$E_L = \frac{1}{2} * 22.9\mu H * \left(58.7A * \sqrt{2}\right)^2 = 0.08J$$

The quality factor is then:

$$Q = 2\pi * 120kHz * \frac{80mJ}{1kW} = 60.3$$

Matching Transformer:

The design goal of the matching transformer was to match the resistance presented by the resonant tank to an impedance that could be easily driven from an inverter operating with a commonly-available DC bus voltage. This design is based on operation at an average bus of 120VDCto allow for operation with rectified 120VAC with minimal filter capacitor for line ripple. The IH circuit was designed to be able to operate as natural power factor correction. The

main consideration in the transformer design was in reducing losses in the high-current secondary. After testing experimental designs, it was found that losses in the secondary winding were more difficult to mitigate than primary winding or core losses (the core used is oversized for this power level). The transformer was constructed using E-80 size cores made of 3C94 ferrite material from Ferroxcube, Inc. A low turn count was attempted in order to minimize losses in the secondary winding. The core was assembled with no air gap in order maximize magnetizing inductance so that a lower turn count could be used without causing excessive magnetizing current. This does however pose the issue that without an air gap, the core can be easily driven into saturation. Because of this, it becomes absolutely necessary to block any DC offset from the inverter. Three paralleled 20µF polypropylene film capacitors were connected in series between the inverter and transformer primary for the purpose of DC blocking.

Selecting transformer turns-ratio for proper operation in the absence of closed-loop control posed a challenge due to the high-Q nature of the load. Because of this characteristic, the transformer is required to output a high enough voltage do drive the load with desired power even when a somewhat-reactive impedance is presented. Delivering 1kW into a real 290mΩ resistance would only require $17V_{rms}$. From previous experimentation, it was determined that the transformer should be designed to output at more than 20% higher than the theoretical value for a purely resistive load ($20.4V_{rms}$) in order to overcome the additional reactive impedance and transformer impedance/losses. An output of 20.4V minimum with 120V input requires in a ratio of 5.88:1 or smaller. In attempt to minimize the number of turns in the high-current secondary, it was wound with 3 turns. A primary turns-count of 17 resulted in a ratio of 5.67:1 and was experimentally found to provide a large enough magnetizing inductance. The transformer is shown in figure 5.4.

The primary of the transformer was wound with 17 turns of 12AWG-equivalent, 44AWG-stranded Litz wire. The secondary was wound with 3 turns of 3-paralleled 10AWG-equivalent, 44AWG-stranded Litz wire. The magnetizing inductance reflected at the primary was measured to be 1.30mH @ 100kHz. With a 120VDC bus, magnetizing current at the 120kHz fundamental is then expected to be 122mA.

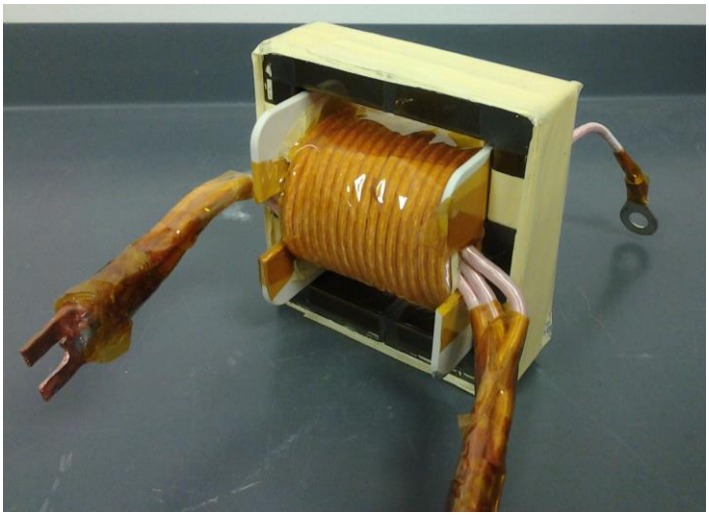

Figure 5.4. Matching Transformer (17:3 turns-ratio)

Inverter:

Unlike most on-the-market induction cookers which use IGBTs as the main power stage switches for robustness in loss-of-ZVS conditions, this design uses MOSFETs in an attempt to improve inverter efficiency if soft-switching conditions can be maintained. A full-bridge inverter (figure 5.5) was built using Fairchild FCH76N60NF (600V, 28.7mΩ typ., 38mΩ max.) MOSFETs with analog variable-frequency control. A fixed dead-time of 400ns was used to support zero-voltage turn-on when operating near resonance (low switch current at commutation). The gate drive topology consisted of four individual gate drive ICs and four transformers that provided both power and gating signal to the gate drivers. The gating signal, driven with sufficient current, is supplied to a gate drive transformer. The output of the

transformer is used to provide the control signal to a non-isolated gate driver. The transformer output is also rectified and used to charge a capacitor that provides power to the gate driver. Although not novel, this topology is not widely employed. This topology offers a means of driving the gate with only one point of isolation for each device, unlike other designs which require an isolated supply and signal isolation. Unlike a conventional transformer gate drive, the active gate driver is directly connected to the gate of the device, offering improved performance and without the impedance and parasitics of a transformer. Unlike a boost-strap configuration, gating is not dependent on switch-node voltage at startup, however proper gating cannot be achieved until the gate drive has been operated for a few cycles to charge the gate drive floating supply capacitors. This inverter used 1:1 transformers driven with 12 volts to provide a gate drive of approximately 10 volts after losses.

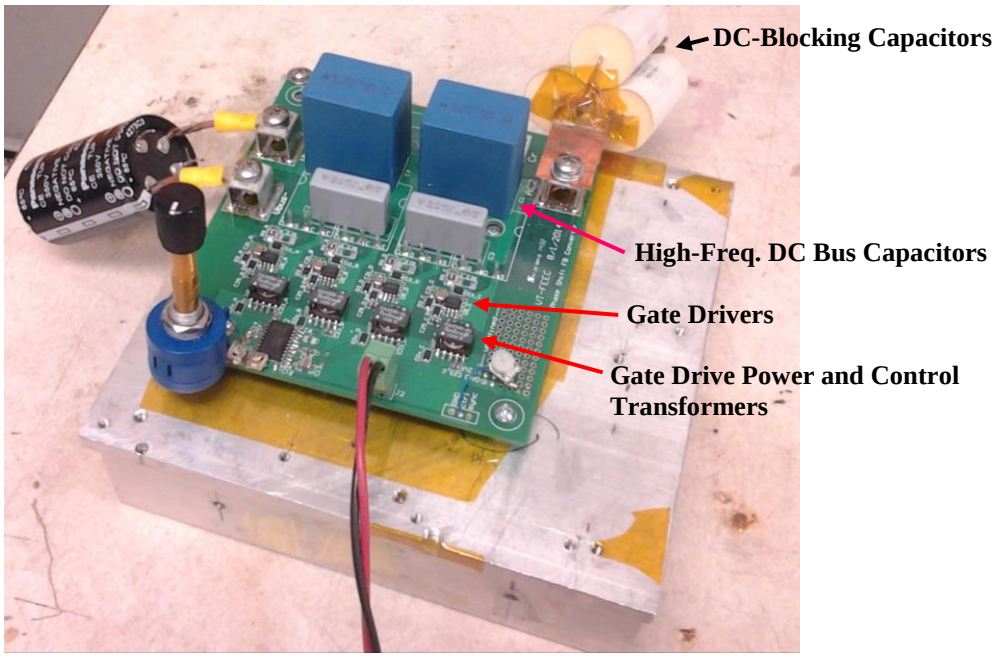

Figure 5.5. Full-Bridge MOSFET Inverter with Variable-Frequency Drive Circuit (mounted on heatsink)

The circuit was operated at a frequency where the transformer presented a slightly inductive load to the inverter to allow for the resonant current to fully charge and discharge

device capacitances within the 400ns dead-time interval and provide zero-voltage turn-on of the MOSFETs. Switching waveforms were observed via oscilloscope to verify zero-voltage switching. Output power was then controlled by further adjusting the switching frequency above coil/tank resonance. The limitation of any continuous-operation-mode (as opposed to pulsed or burst-mode methods) is that the reduction in resonant current results in a slower charge/discharge rate of device capacitances and makes zero-voltage turn-on more difficult to achieve. The use of frequency-based control has an advantage over duty-cycle-based methods in that the increased phase shift between voltage and resonant current as power is reduced results it commutation occurring at a higher point in the current waveform. The higher switch current causes more rapid charging of device capacitances and supporting zero-voltage turn-on. There is some loss of efficiency associated with this approach due to higher switch turn-off losses and increased body diode conduction period and current. The transformer-coupled topology further supports zero-voltage switching at low power levels as the magnetizing current of the transformer reaches its peak value near the time of commutation and is approximately constant over the frequency range associated with power control.

Cooling:

A cooling blower was used to force air through the gap between the coil and insulation as well as through the gaps in the E-cores on the underside of the ferrite assembly. Another fan was mounted to blow air over the resonant capacitors and transformer. The inverter MOSFETs were mounted on a large heatsink with no forced-air cooling. This cooling configuration was used throughout the experimental operation presented in this work.

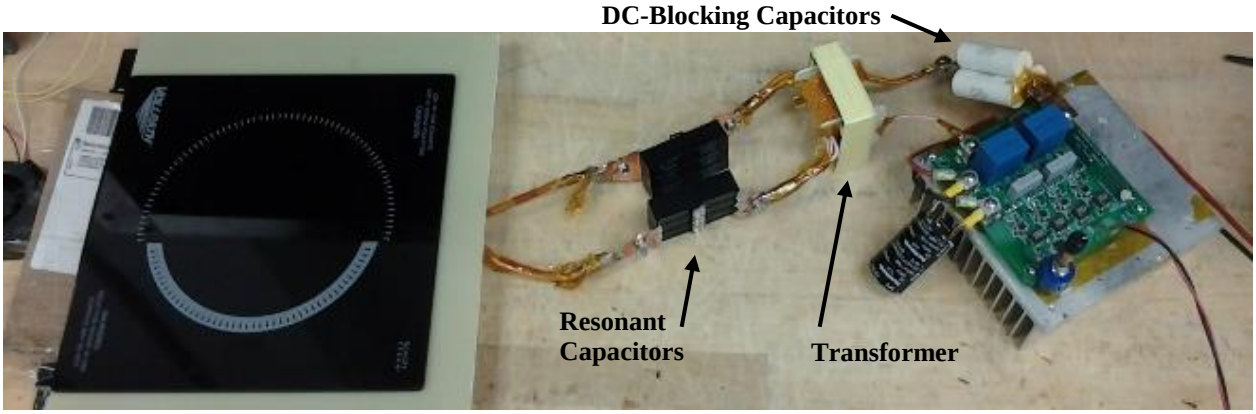

Figure 5.6. Experimental Transformer-Coupled Induction Cooker Circuit

Experimental Results

A measured inverter output power of 1.07kW was achieved when operating the circuit at 120kHz with a bus voltage of 120VDC. Power was measured via oscilloscope over approximately 30 switching cycles. Further increasing the supply voltage to 170VDC yielded an output power of 1.66kW. At this operating point, the coil current was $73.7A_{rms}$ and the voltage across the coil was $1.29kV_{rms}$. The transformer primary current supplied by the inverter was 13.1A. Further increase of output power was limited by coil and ferrite heating and by maintaining a margin of safety on resonant capacitor voltage.

Circuit waveforms from the 1.66kW operating point at 120kHz are shown in figures 5.7 and 5.8. As can be observed, the coil current and transformer primary current (inverter current) are sinusoidal as the circuit is operating near resonance and resonant component of the circuit impedance is significantly larger than the real resistive element. At ambient temperature, the resonant frequency observed at the transformer primary terminals was 118kHz (lower than that of the main resonant tank). As the coil and resonant capacitors came up to operating temperature, the resonant frequency increased and the 120kHz operating point was close to this resonance. The transformer output voltage waveform is significantly distorted due to the transformer leakage inductance and the large resonant current. The coil current is leading the transformer output voltage, whereas the primary current to the transformer is lagging the inverter output voltage. Here, the resonant tank is actually operating in a capacitive region slightly below its resonant frequency. When this impedance is combined with the magnetizing and leakage inductances of the transformer, the load presented to the inverter is inductive.

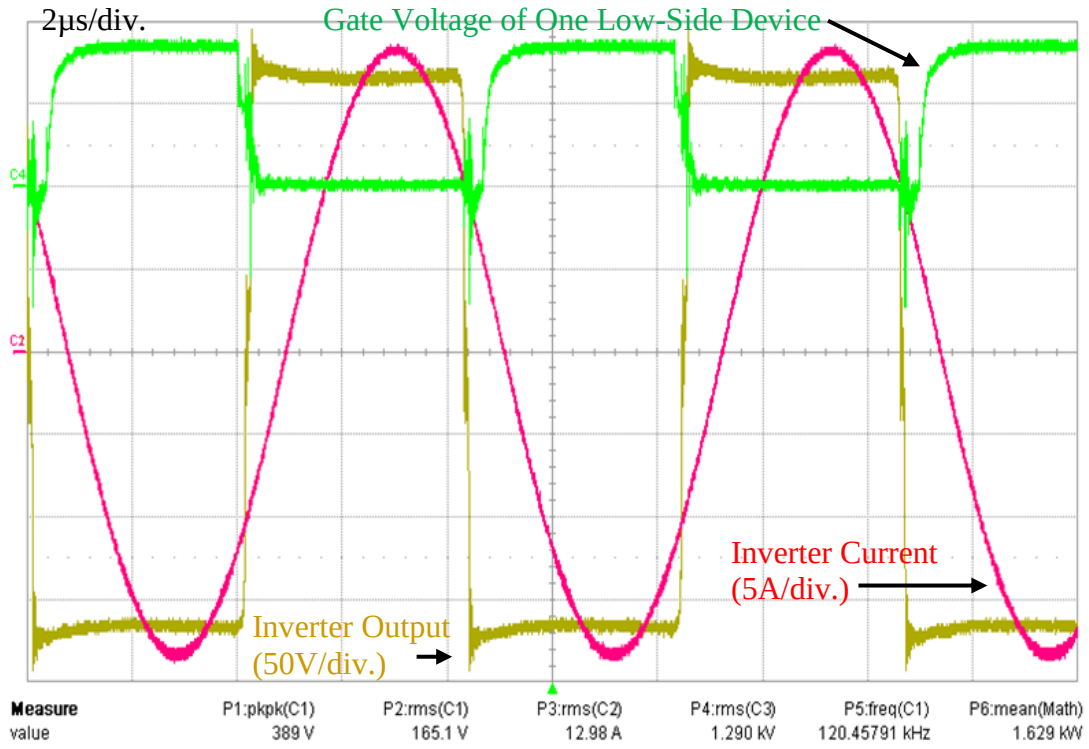

Figure 5.7. Transformer Primary-Side Waveforms for Operation at 120kHz and 1.66kW
(All 2µs/div.)

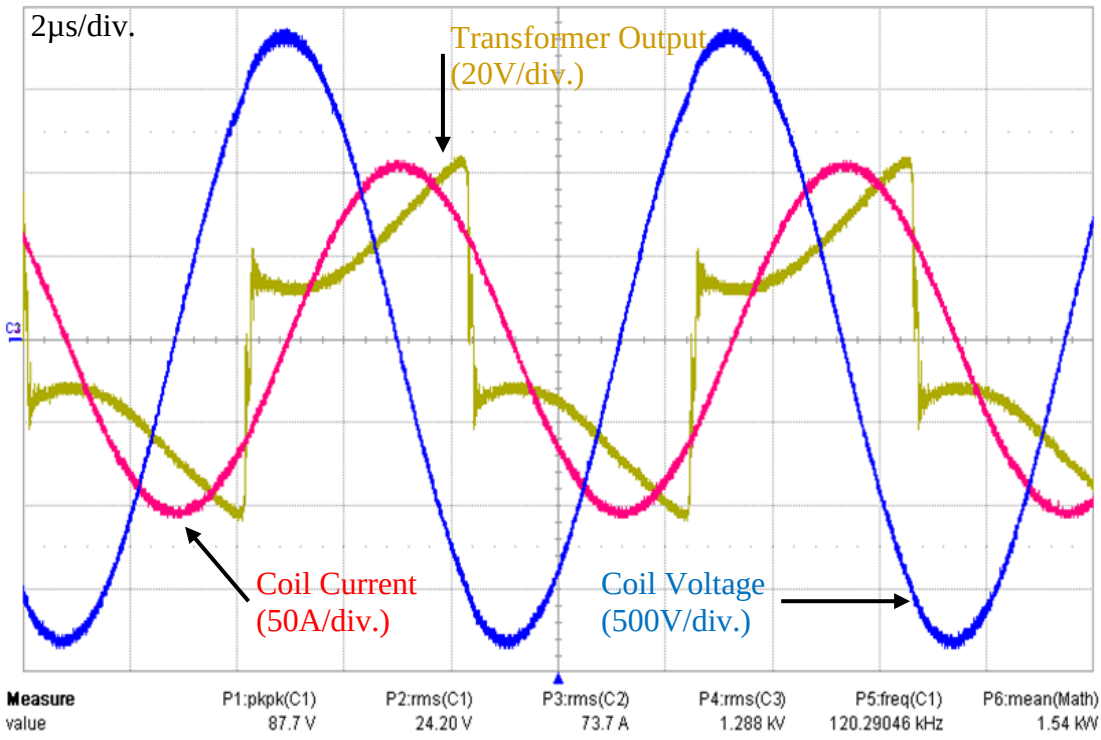

Figure 5.8. Transformer Secondary-Side Waveforms for Operation at 120kHz and 1.66kW
(All 2µs/div.)

The inverter is achieving zero-voltage turn-on as evidenced by the clean gate signal on turn-on in figure 5.7 and supported by the current lagging the output voltage. However, some gate oscillation and switch-node overshoot are observed during turn-off due to high dv/dt. A portion of this observed behavior is likely due to ringing in the oscilloscope probe and not actually experienced by the inverter. As shown in figure 5.7, the inverter is not operating near unity power factor. When operated with less of a phase lag between voltage and current, the MOSFETs were not fully turned-on at the time of current crossover. A fixed 400ns dead-time was implemented to provide an extended zero-voltage turn-on range at low power operation. However, this adds to the turn-on delay of the MOSFETs and sets a minimum time between the turn-off of one pair of switches and time at which a conducting channel is fully established in the complementary pair. Here, the limitation is not in fully discharging device capacitances before switch turn-on, but in fully turning-on the switch before current commutation. It should also be noted that the transformer-coupled gate drive circuit is only driving the devices with less than 9 volts (figure 5.7). With a 12-volt gate drive supply, this is a 25% effective driver conduction drop. The gate drive circuit was originally designed for IGBT operation at this frequency and became inefficient under the load posed by the increased capacitances of the MOSFET gating. The low gate voltage did not pose a severe operational problem in this case, although the MOSFETs are likely not achieving their specified on-resistance. Operating conditions are summarized in table 2.

Table 2: Transformer-Coupled IH Experimental Test Parameters

Switching Frequency	120kHz
Maximum Power	1.66kW
Coil Current (@ max. pwr.)	73.7A
Coil Voltage (@ max. pwr.)	1.29kV
DC Bus Voltage (max. pwr.)	170VDC
Min. Power for ZVS Operation	<250W

The High-Q characteristics of the resonant tank were observed both in the frequency sensitivity to power control and sensitivity to temperature variation of resonant elements. Increasing the switching frequency by less than 2kHz above the original operating point resulted in a reduction of output power to 250W (15% of the original value). The large circulating currents at reduced power allowed for zero-voltage switching to still be maintained at this operating point. As the coil/ferrite and resonant capacitors came up to operating temperature from ambient conditions, the drift in resonant capacitor value and in coil/ferrite inductance caused an increase in resonant frequency significant enough to require frequency adjustment to maintain constant power and zero-voltage switching conditions. A relationship of DC bus voltage to output power has not been investigated in this work, as the variation in operating point of the open-loop system does not allow for consistent accurate measurement.

Although quantitative measurement has not been performed, the Lorentz forces acting between the pan and coil are not pronounced enough to lift or move the pan at this power level. Another observation was that metal objects in close proximity to the coil leads, resonant capacitors, and transformer secondary experienced eddy-current heating from the stray flux.

After 10 minutes of operation at full power, the temperature of the coil was 105ºC. Temperature was measured by inserting a thermocouple between the coil and cooktop insulation immediately after shutting down the circuit (air gap small enough that thermocouple pressed against coil). Temperature measurement was not possible during operation due to interference to and induction heating of the thermocouple itself. The hottest part of the ferrite shielding occurred where flux was most concentrated at the center and in the side pieces. The highest measured temperature was 98ºC. The windings were the hottest part of the matching transformer, which were 41ºC. The resonant capacitors reached a temperature of 46ºC.

VI. ZERO-VOLTAGE DETECTING INVERTER APPLIED TO TRANSFORMER-COUPLED TOPOLOGY

The use of MOSFETs allows for potential efficiency improvement over IGBTs in domestic induction cooking devices. The main obstacle to the use of MOSFETs is the loss of efficiency if zero-voltage turn-on is not maintained and their lack of robustness in such conditions. When soft-switching conditions are not achieved, the turn-on loss of the MOSFET often dominates the overall device loss breakdown. Induction heating applications pose a challenge in that resonant conditions can change severely with movement of the work piece (cooking vessel in this case). Most earlier induction cooking devices did not have any means of closed-loop control to ensure soft switching and therefore required a higher degree of switch robustness during unusual conditions and startup. A full-bridge inverter with switch voltage detection circuitry was built and tested to evaluate the feasibility of a MOSFET inverter using active zero-voltage control. Analog circuitry was implemented to directly inhibit gating when switch voltage was above a threshold, reducing the processing load and performance requirements of the microcontroller.

The experimental induction cooker circuit was also designed with several improvements over previously-presented work in the interest of building a practical prototype aluminum-compatible induction cooker. On issue encountered was that stray flux from the high-current coil, capacitor, and transformer-secondary circuit coupled to nearby objects, causing eddy current heating and electrical interference. Additional considerations were taken to minimize and shield the high-current loop. This inverter also included a front-end rectifier and small, non-smoothing DC bus capacitors for operation with an AC supply and natural power-factor

correction. An on-board auxiliary power supply was also included. Current sensing circuitry was implemented for both the inverter output and the AC supply for control purposes.

In the previously built and tested IH circuit, the large-diameter coil worked efficiently for large pans, but encountered problems in heating smaller cooking vessels. When a pan of smaller bottom diameter than the coil was used, the reflected resistance decreased due to fewer turns of the coil being coupled to the pan and the leakage inductance of the coil increased due to the reduced coupling. The decrease in resistance does not pose a severe problem if reduced output power is acceptable when heating smaller pans. The increased leakage inductance impacts the resonant frequency of the circuit but this is not a major problem if frequency-tracking control is employed. The increased inductance however also results in a significant increase in resonant voltage, adding to the voltage requirement of the resonant capacitors. The other problem with a cooking vessel smaller than the work coil is that the coil also couples to handles and other external hardware, causing unwanted heating. For this design, a smaller-diameter 2-layer interleaved coil was used to improve compatibility with smaller vessels.

Design and Construction of Experimental Circuit

The switch-voltage detection circuit consisted of an isolated DC-DC converter, an optocoupler, and a high-voltage diode connected across the switch as shown in figure 6.1. When the voltage across the switch is low, the isolated DC supply forward-biases the emitter of a high-speed optocoupler, which provides the logic signal to the gating circuit. A high-voltage diode was used to block high switch voltage from this circuit. This voltage detection circuit was implemented on both lower switches in the inverter. One isolated DC-DC supply was used to drive both circuits, as they both share the negative DC bus. The gating scheme for this inverter

drives the diagonal pairs of switches together. Here, the voltage across the lower switches is assumed to be an accurate reflection of the voltage across their upper-diagonal counterparts.

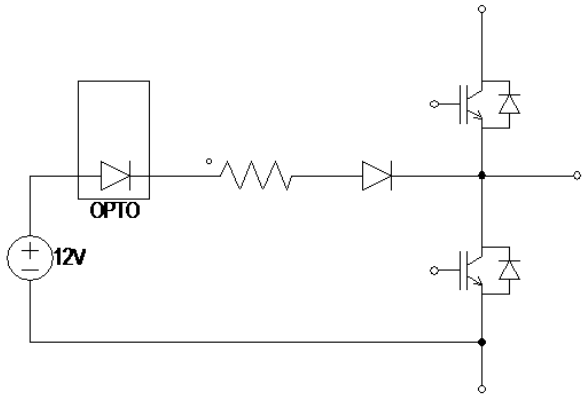

Figure 6.1 Switch Voltage Detection Circuit

The switch voltage detection circuit was used to provide an external output for future microcontroller/DSP interface, as well as controlling an analog gating-inhibit circuit. A hard-wired analog gating-inhibit circuit was used so that the switches could be turned-on at zero-voltage conditions without any interaction with additional control. The analog circuit allows for high-speed response without posing high-performance real-time response requirements on a microcontroller or DSP. In order to allow for more flexibility in startup schemes and due to the gate voltage issues encountered in the transformer-controlled/powered gating of the previous design, RF-isolated gate drivers powered by isolated DC-DC converters were used on all four switches.

The full-bridge inverter (figure 6.2) was built using IPW60R041C6 MOSFETs (600V, 41mΩ) from Infineon Semiconductor. The inverter also included a full-bridge rectifier for operation from an AC power source. The DC bus capacitance consisted of two 4.7μF polypropylene film capacitors. This capacitance filters the twice-switching frequency current ripple but allows for high power factor when supplied with line-frequency AC through the full-

bridge rectifier. Current sense transformers are used on both the inverter output and the AC line input to the inverter to provide feedback to a future controller. The transformer on the AC line is connected to a passive rectifier and smoothing filter to provide a DC output approximately corresponding to input current for power control purposes. The transformer on the inverter output is connected to an active peak magnitude detector for resonant current monitoring and also to a slope-detection circuit to allow a simplified digital means of resonant frequency tracking. The DC-blocking capacitors on the inverter output were located on-board. This consisted of three parallel 3µF 400V polypropylene film capacitors. An on-board auxiliary supply was used to provide power to gating, on-board analog control, and coil/tank cooling fans.

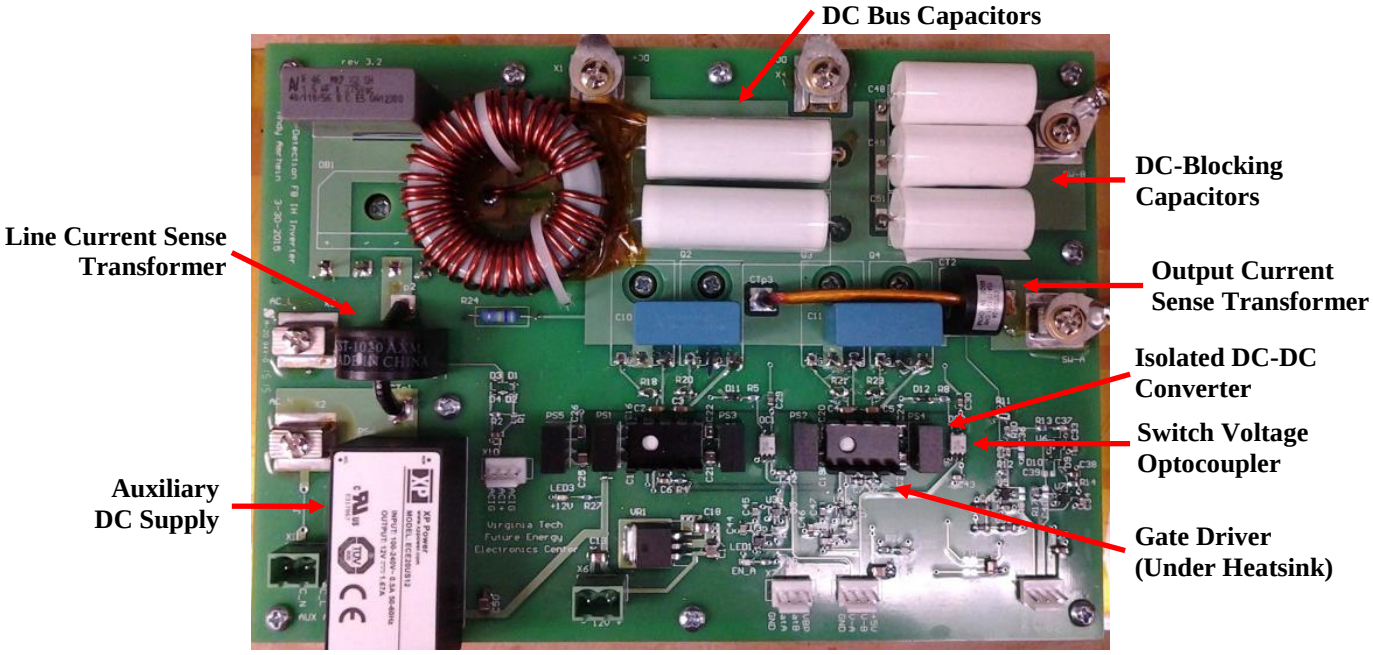

Figure 6.2 Zero-Voltage-Detecting Full-Bridge IH Inverter

To overcome the problem of coil coupling varying significantly with the size of the cooking vessel, a smaller diameter work coil was used. The coil used in this experimental unit consists of 23 turns of #9AWG-equivalent, #46-AWG-stranded type-2 Litz wire in a two-layer interleaved winding pattern. This coil has an outer diameter of 185mm, as compared to the

234mm diameter of the single-layer coil in the previous design. The coil was mounted on a 5mm-thick tiled ferrite sheet made of MN80C material from Ferroxcube, Inc. Additional ferrite pieces were added around the edges of the coil to improve coupling to the pan.

The coil and ferrite assembly was epoxied to FR4 board as shown in figure 6.3. The resonant capacitors and matching transformer were mounted directly under the board with minimal loop length on the high-current coil-capacitor-transformer secondary circuit as shown in figure 6.4. The same 3-parallel, 4-series combination of 100nF, 460VAC capacitors from the previous design was used. The resonant frequency is reduced to 108kHz due to the increased effective inductance of the 23-turn 2-layer coil. The primary winding of the matching transformer was reduced to 16 turns from the previous 17-turn design. The ratio was modified in order to allow for high-power operation when operating further away from resonance in order increase ease of control. A small air gap was allowed above the coil and side ferrite pieces for cooling. A blower was mounted under the assembly to force air up through the center of the coil and through the gap. Figure 6.5 shows the entire assembled system.

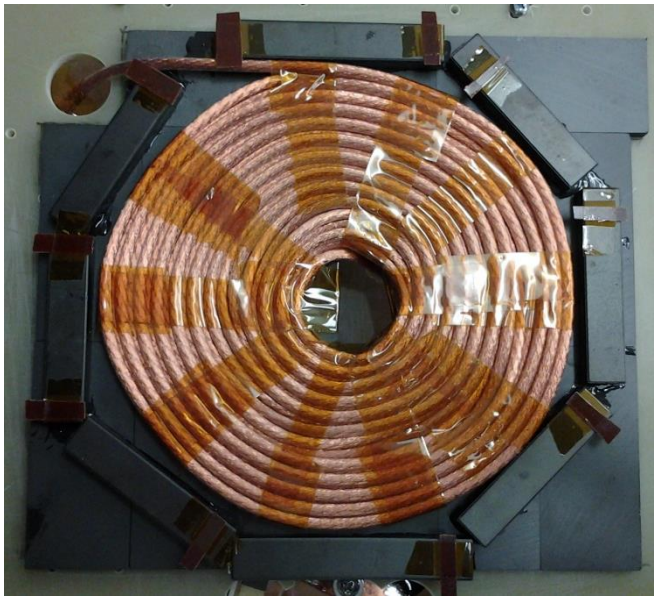

Figure 6.3 23-Turn 2-Layer Work Coil Mounted on Ferrite Sheet

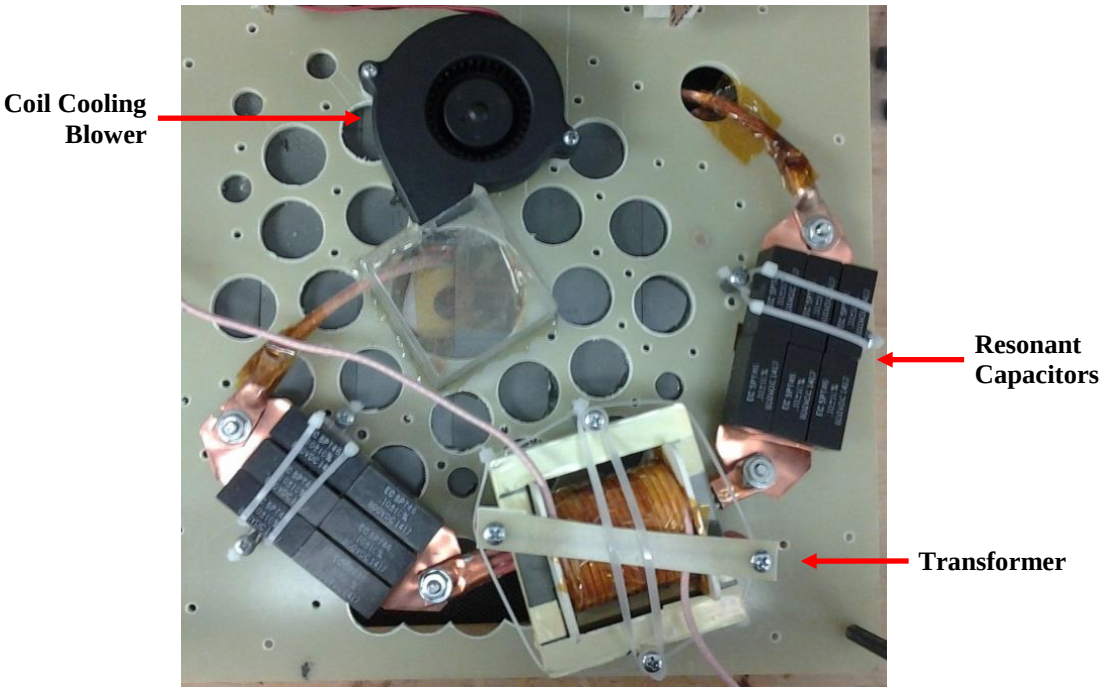

Figure 6.4 Underside of Coil Assembly

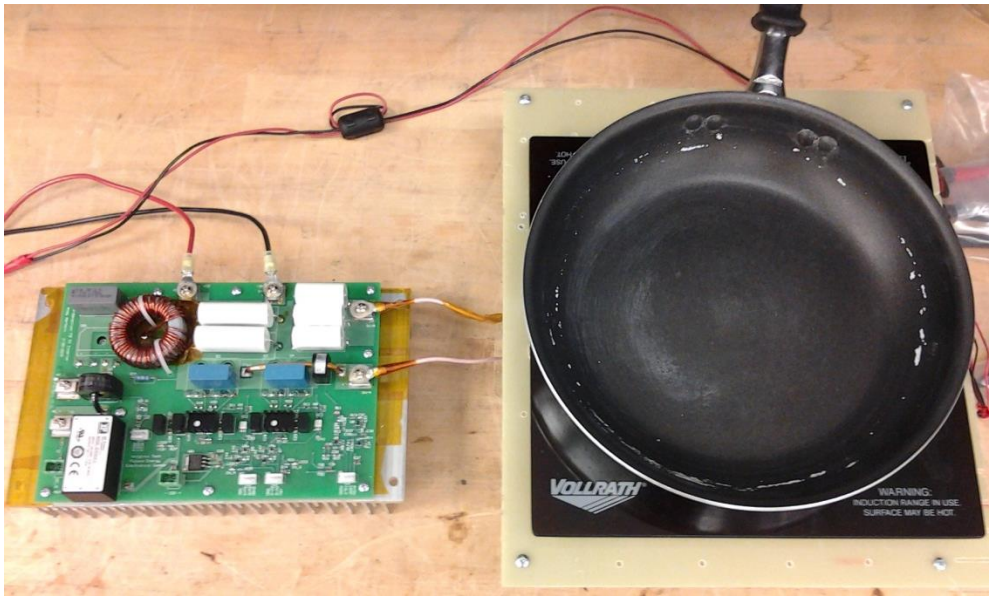

Figure 6.5 Induction Cooker Circuit with Zero-Voltage-Detecting Inverter

Preliminary Experimental Results

For initial testing of the zero-voltage-detection and analog gating control, the inverter was operated with a DC supply. No additional control beyond the analog zero-voltage gating was

used in this test. The two gating inputs were driven with complementary 50% duty-cycle signals. The circuit was operated above its 108kHz resonance and frequency was varied to control power.

Inverter waveforms for experimental operation at 1.4kW with a 150VDC bus are shown in figure 6.6. The shown switch voltage, gate voltage, and switch voltage detection logic signal (low when switch voltage below threshold) all pertain to the same low-side switch. The 300ns deadtime between low-voltage detection and gate turn-on can be observed in the switch-voltage-detection and gate voltage signals. Zero-voltage turn-on is being achieved as evidenced by clean voltage transition and gate signals. The inverter output current is not in-phase with output and switch voltage as this delay requires a phase shift between output voltage and current in order for current commutation to occur after the switch is turned-on.

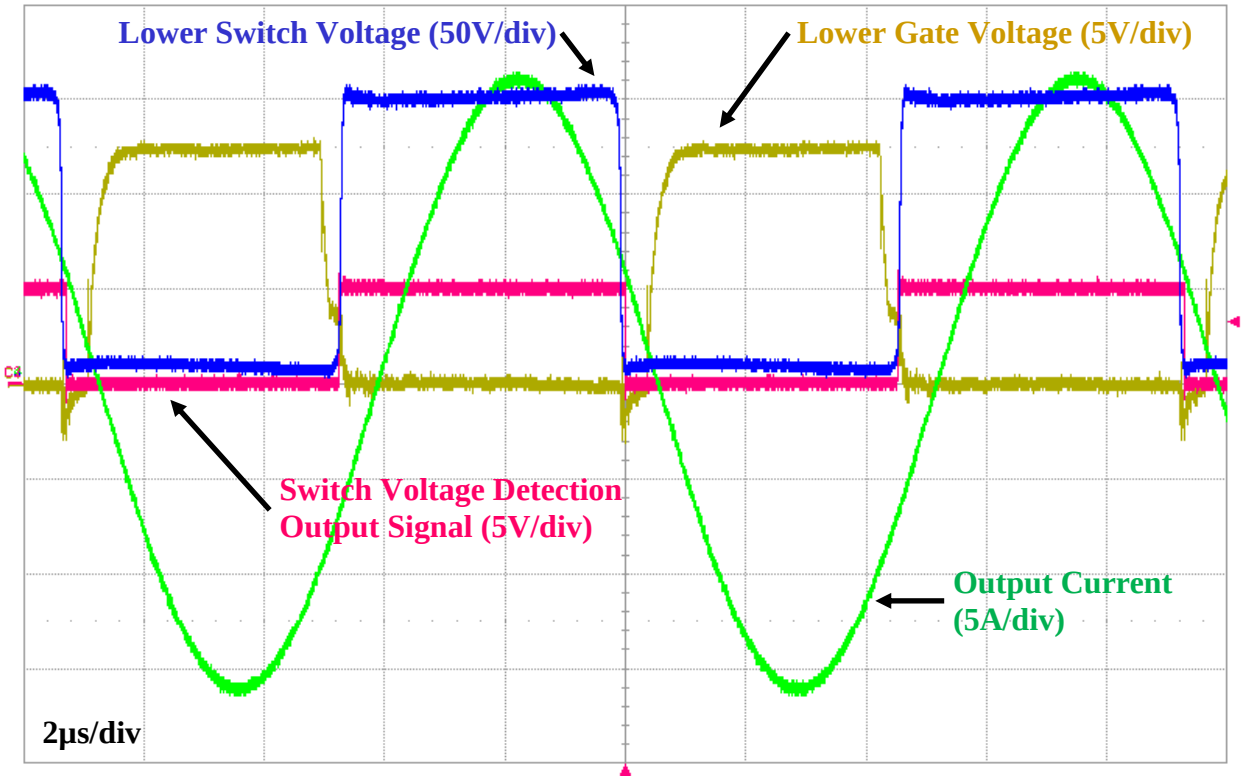

Figure 6.6 Inverter Waveforms for ZVS-Detecting Inverter Operating at 1.4kW and 108kHz at 150VDC

The operation of the inverter switch-voltage detection with the inverter operating at 1.2kW with a 120VDC bus is shown in figure 6.7. Initially, the upper switch is on and the lower switch voltage is high. When the upper switch turns off, the transformer input current charges device capacitances and the lower-switch voltage falls. The switch voltage detection signal goes low when this voltage drops below approximately 10 volts. Upon this low-switch-voltage signal, the gate is driven high after a 300ns delay. The device is turned-on by the time that the current crosses over.

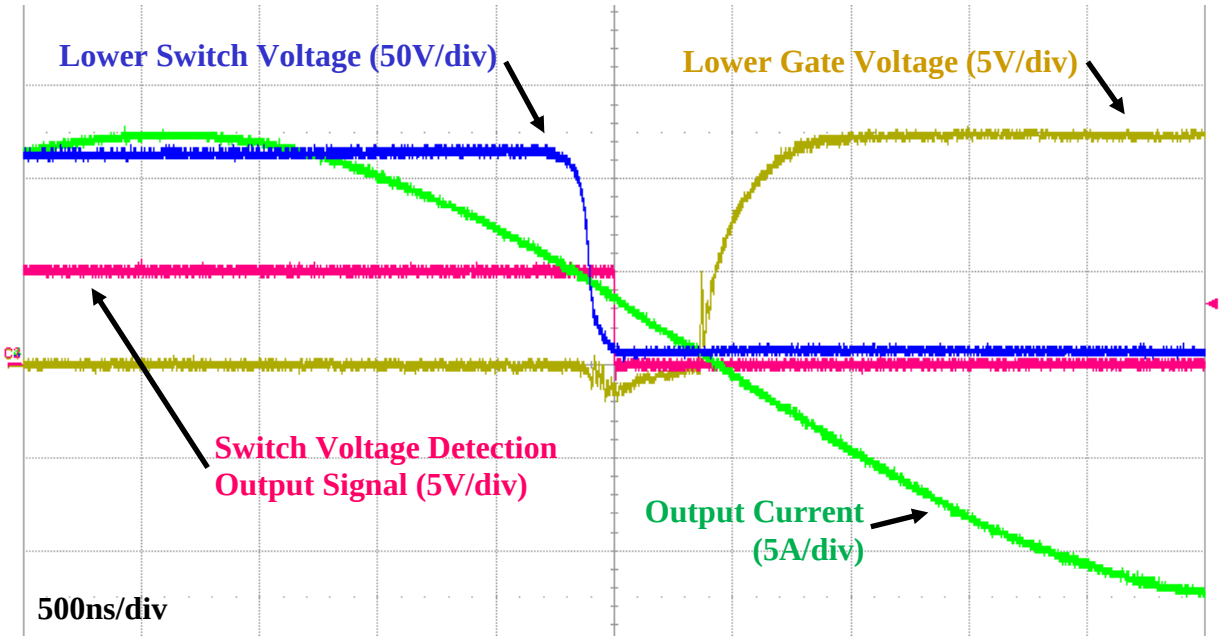

Figure 6.7 Operation of Switch Voltage Detection at 1.2kW IH Operation

Without any intelligent control being implemented, there are a few cases where the analog zero-voltage control causes the circuit to become unstable, although not posing any risk of damage to the inverter or load. If the circuit is operated close to resonance where zero-voltage turn-on requires a significantly increased delay before switch turn-on, the resulting reduction of duty cycle causes a condition where resonant current is unable to discharge device capacitances and the circuit either stops switching or switches at a discontinuous interval. A similar issue

occurs during startup where the resonant current is initially to low to discharge device capacitances and permit switching. This issue can be overcome by starting the circuit well above resonance so that switch current is higher at turn-off, providing higher device charging capabilities.

Future work and testing (not included in this thesis) involves operating the circuit from an AC power source, adding digital control, and using the digital control to implement start-up and protection operations.

VII. SUMMARY AND CONCLUSIONS

Induction heating of aluminum and copper cookware is difficult due to the low reflected resistance caused by low resistivity and lack of ferromagnetic properties (no hysteresis heating). Various techniques, technologies and circuit topologies have been developed for this application with varying degrees of success. Although several designs accomplish the task of heating low-resistivity cookware, they are often limited by practical implementation, size, cost, and/or esoteric component requirements.

Increasing the number of turns on the induction work coil results in an increased reflected resistance. However, it also increases the AC losses in the coil and results in an increased resonant voltage, potentially on the order of kilovolts or tens of kilovolts for aluminum IH applications. Devices have been patented which consist of a conductive structure that interacts with the magnetic flux from the coil and focuses it on a smaller region of the cooking vessel, increasing the effective resistance. The problem is that this metal structure experiences significant eddy-current heating itself, reducing overall efficiency if there is not a thermal path to the stovetop and cooking vessel. Here, heating of the cookware is not carried out entirely by induction heating. When operating at high frequencies, skin effect causes an increase in the effective resistance of the metal being heated. However, losses in the coil also increase with frequency and inverter capabilities put a limit on practical switching frequency. Multiple topologies have been proposed and implemented that operate the induction load at a multiple of the switching frequency to overcome the issue of limited switching frequency. A multi-resonant circuit consisting of a series-resonant coil/tank driven by a single-ended IGBT and DC link inductor leg can be operated as a frequency doubler when switched at half of the resonant

frequency of the series-resonant tank. The limited control capabilities can be improved by a time-sharing topology consisting of two single-ended legs capacitively coupled to the series-resonant load. This involves a much higher passive component count and still only operates the coil at twice the switching frequency. In a similar approach to the frequency doubler, a topology consisting of two sets of parallel coil windings driven out-of-phase by two inverters was proposed to increase the effective operating frequency. This reduces inverter losses and the losses in each winding as they are operating at half of the effective output frequency. However, the double windings reduce the turns-density of the coil. In harmonic operation, a series-resonant circuit can be operated at an odd harmonic of the switching frequency. Because of the amplitude of harmonics relative to the fundamental, this also results in an effective voltage step-down ratio, allowing for impedance matching to the low-resistance-coupled coil. By selecting the harmonic of switching frequency used (changing switching frequency or switching between resonant capacitors), the matching ratio can be adjusted. The downside to this approach is the large amount of circulating power. Due to the circulating power, the inverter operates at low power factor and body-diode conduction is inherent in a significant portion of the switching cycle, limiting efficiency. The high reactive power also increases losses and component requirements in the resonant tank.

A high-frequency inverter was built in order to evaluate the feasibility and efficiency of operating an induction cooker with aluminum load at frequencies up to 1MHz. At this frequency, skin effect resulted in a greatly increased reflected resistance from the pan. However, the AC losses in the coil also increased greatly, resulting in poor efficiency. The efficiency of the aluminum-coupled coil was found to be less than 60% based on resistance measurements.

The impedance of the coil can also be matched to the inverter by means of an L-C matching network or transformer. The matching characteristics of the L-C network are dependent on frequency and load impedance. Although this allows adjustment to be made solely by frequency variation, it causes problems when attempting to match to different impedances with different resonant frequencies when pans of different composition and sizes are used. Although limited to a fixed ratio without tap-changing, a matching transformer allows for a specific ratio that is consistent over all operating conditions. Due to the large amount of reactive power in the resonant tank, is preferable for the transformer to drive a conventional series-resonant tank as opposed to the transformer being part of the tank.

A transformer-coupled, series-load-resonant topology was proposed, built, and experimentally evaluated as an efficient means of induction heating low-resistivity cookware. This topology uses a conventional series-load-resonant circuit consisting of a planar work coil mounted on ferrite shielding and series-connected resonant capacitors. The resonant circuit is then coupled to a voltage-sourced inverter by a matching transformer, which allows for the low coil resistance to be easily driven by a practical inverter. The transformer is driven by a full-bridge MOSFET inverter. The inverter was based on MOSFETs in order to evaluate the viability of their use in induction cooker applications as they can potentially be operated with less loss than IGBTs in this application if zero-voltage switching is guaranteed. Measurements of coil efficiency indicated that out of the coil designs tested, the most efficient coil was a 22-turn planar design operating at 140kHz. A series/parallel combination of resonant capacitors was used to give a resonant frequency of 120kHz while maintaining sufficient current and voltage capabilities. The circuit was operated at a frequency where the primary of the transformer

presented a slightly inductive load to the inverter in order to charge device capacitances within the dead-time interval and provide zero-voltage turn-on.

The operation of the transformer-coupled circuit was successfully verified with an output power of 1.66kW sustained for an extended period of time while operating from a practical supply voltage. The initial design power of 1kW was achieved under the design conditions. Higher power was achieved by increasing the DC bus voltage above the original design value. Further increase of output power was limited by coil temperature and by maintaining a safety margin on resonant capacitor voltage. The majority of losses were in the work coil. Relationships of frequency-to-output power and supply voltage-to-output power have not been investigated in this work as the high-Q nature of this circuit did not permit a stable operating point without closed-loop control. Also, Lorentz forces between the coil and pan were not pronounced enough to lift or move the pan at this power level.

Output power of the system was measured as the power delivered to the transformer and resonant tank by the inverter, which includes coil, transformer, and resonant capacitor losses as well as power actually delivered to the pan. The coil design used in this experimental circuit was found to have a maximum efficiency of 86.9% at the optimum frequency of 140kHz. Due to the amount of power dissipated in the coil, optimization was critical to the functionality of the system. Since the coil impedance was not restricted by inverter parameters due the transformer matching, it was possible to design the coil for optimal efficiency with less electrical restrictions.

Conclusions:

A proposed transformer-coupled series-load-resonant induction cooker topology was built and its operation was successfully verified for the heating of an aluminum pan. It was able to deliver an output power comparable to that of domestic ferromagnetic induction cookers while operating in a supply voltage range that was practical for this power level. The impedance matching freedom offered by the transformer coupling also allowed for the work coil to be designed for optimal efficiency without being limited my other circuit constraints. The successful implementation and test of the topology under practical limitations demonstrate the viability of using a transformer-coupled topology to accommodate the low reflected resistance that is characteristic of an aluminum cooking vessel. Additional work is needed to verify the cause, but an initial conclusion is that the increased resistivity of the pan due to skin effect reduces Lorentz forces enough to prevent levitation on the pan.

This topology exhibits advantages over most of the existing designs for heating low-resistivity cookware. The available matching ratio allows for a reduced number of turns in the work coil, where other all-metal designs relied on a high number of turns to reflect the desired resistance. In addition to improved coil efficiency, the low turns count also results in lower resonant voltage, allowing for more practical capacitor designs and reducing safety challenges. Transformer-matching yields improved inverter efficiency over harmonic operation methods due to lower circulating energy. When operating in harmonic mode, the inverter operates at low power factor and body diode conduction is inherent. When driving the transformer, the inverter operates at high power factor and body diode conduction can be eliminated at a certain operating point. Also, the reduced circulating energy results in less stresses and losses in resonant elements and therefore less extreme component requirements.

One limitation of the transformer-coupled topology as presented is inability to adapt to heating cookware made of high-resistivity and/or ferromagnetic materials. Because it is designed around the low resistance presented by an aluminum cooking vessel, the circuit is unable to deliver reasonable power into the high resistance reflected by a steel or iron pan and resonant current is too low to support zero-voltage switching. One method of solving this problem is to switch between multiple taps on the transformer secondary. The problem with this though is that the high secondary currents are not practical for the use of a conventional relay. It should be noted though that all of the frequency-doubler and harmonic operation topologies analyzed also used relays to switch different capacitors into the high-current resonant circuit when adjusting between high- and low-resistivity cookware.

The output power was measured as the power supplied to the transformer by the inverter. In actuality, this includes losses in the coil, transformer, and resonant capacitors in addition to the power delivered to the pan. Using the measured coil efficiency of 86.9%, the power delivered to the pan was 1.44kW neglecting transformer and resonant capacitor losses. It should be noted though that the marketplace power ratings of most induction cookers are actually measured as the input power to the inverter and neglect both inverter and coil losses. Most of the losses observed in this circuit were in the work coil, further enforcing the need for optimal coil design. The control over matching ratio offered by the transformer is favorable in that it allows the circuit to be designed around the coil impedance, putting less electrical restriction on coil optimization.

The high-Q nature of the aluminum-coupled resonant tank is sensitive to frequency variation and resonant component drift, posing a few control challenges. The controller must have high frequency resolution in order to maintain stable and accurate control of the system, as

small incremental changes in switching frequency have a large impact on circuit operation. Also, the controller must be able to continuously track resonance and the desired operating point as changes in resonance due to temperature-related component drift will impact the operating point by a large degree if frequency is kept constant.

The use of a MOSFET inverter has been successfully tested when operated under zero-voltage turn-on conditions. Previously most designs used IGBTs for robustness under loss of soft switching, such as with some cookware-dependent resonant conditions, during startup, and when cooking vessel is moved or removed during operation. The use of MOSFETs could potentially have significant efficiency benefits. However, the controller must ensure zero-voltage switching conditions in order to avoid damaging the devices. Modern semiconductors also allowed for direct inverter operation at frequencies where previous technologies required a means of multiplication of inverter switching frequency. The magnetizing current of the transformer helps support zero-voltage turn-on of the switches and can be used to provide ZVS conditions even when the operating point of the resonant tank does not support acceptable charging of device capacitances.

Additional evaluation performed using a high-frequency full-bridge inverter in Chapter III demonstrates that a significant increase in IH operating frequency is possible due to improvements in semiconductor technologies. However, this may not be optimal or practical due to reduced efficiency of the work coil and other elements. The experimental circuit was successfully operated at 950kHz but the efficiency of the work coil was measured to be less that 60% at this frequency.

Future/Continued Work:

The transformer-coupled induction cooker topology has been verified as a viable means of heating low-resistivity cookware, however there is likely possibility for further coil efficiency improvement. Additionally, other inverter topologies may provide a more efficient or lower cost means of driving the transformer. The transformer allows for significant freedom in inverter design as the load impedance can be adapted to inverter characteristics. The functionality of a MOSFET inverter was verified when soft-switching conditions were maintained. Additional control schemes and improvements to ensure safe device operation under all conditions have been investigated to some degree. The proposed induction cooker design was not compatible with high-resistivity, ferromagnetic cookware. Additional topological modifications to allow the circuit to adapt to different load impedance have been investigated but have not been implemented at this time.

- Further work coil optimization
- Investigation of alternative inverter topologies to drive transformer
- Control to guarantee safe MOSFET operating conditions
- Power control and startup schemes
- Adaptation to various load impedances (pan resistivity)

REFERENCES

[1] Lucia, O.; Maussion, P.; Dede, E.J.; Burdio, J.M., "Induction Heating Technology and Its Applications: Past Developments, Current Technology, and Future Challenges," *Industrial Electronics, IEEE Transactions on* , vol.61, no.5, pp.2509,2520, May 2014

[2] Bernal, C.; Gaudo, P.M.; Gallego, A.; Otin, A.; Burdio, J.M., "Half-bridge resonant inverter for domestic induction heating based on silicon carbide technology," *Applied Power Electronics Conference and Exposition (APEC), 2012 Twenty-Seventh Annual IEEE* , vol., no., pp.2218,2222, 5-9 Feb. 2012

[3] Hirokawa, T.; Okamoto, M.; Hiraki, E.; Tanaka, T.; Nakaoka, M., "A novel type time-sharing high-frequency resonant soft-switching inverter for all metal IH cooking appliances," *IECON 2011 - 37th Annual Conference on IEEE Industrial Electronics Society* , vol., no., pp.2526,2532, 7-10 Nov. 2011

[4] Hirokawa, T.; Hiraki, E.; Tanaka, T.; Okamoto, M.; Nakaoka, M., "The practical evaluations of time-sharing high-frequency resonant soft-switching inverter for all metal IH cooking appliances," *IECON 2012 - 38th Annual Conference on IEEE Industrial Electronics Society* , vol., no., pp.3302,3307, 25-28 Oct. 2012

[5] Yonemori, H.; Kobayashi, M., "On the Heating Characteristic and Magnetic Flux of a Double-Coil Drive Type Induction Heating Cooker," *IEEE Industrial Electronics, IECON 2006 - 32nd Annual Conference on* , vol., no., pp.2488,2493, 6-10 Nov. 2006

[6] Millán, I.; Puyal, D.; Burdio, J.M.; Acero, J.; Llorente, S., "Resonant Inverter Topology for All-Metal Domestic Induction Heating," *Industrial Electronics, 2007. ISIE 2007. IEEE International Symposium on* , vol., no., pp.913,918, 4-7 June 2007

[7] Millán, I.; Burdío, J.M.; Acero, J.; Lucía, O.; Llorente, S., "Series resonant inverter with selective harmonic operation applied to all-metal domestic induction heating," *Power Electronics, IET* , vol.4, no.5, pp.587,592, May 2011

[8] Fujita, A.; Sadakata, H.; Hirota, I.; Omori, H.; Nakaoka, M., "Latest developments of high-frequency series load resonant inverter type built-in cooktops for induction heated all metallic appliances," *Power Electronics and Motion Control Conference, 2009. IPEMC '09. IEEE 6th International* , vol., no., pp.2537,2544, 17-20 May 2009

[9] Sadakata, H.; Fujita, A.; Sumiyoshi, S.; Omori, H.; Saha, B.; Ahmed, T.; Nakaoka, M., "Latest practical developments of triplex series load resonant frequency-operated high frequency inverter for induction-heated low resistivity metallic appliances in consumer built-in cooktops," *Applied Power Electronics Conference and Exposition (APEC), 2010 Twenty-Fifth Annual IEEE* , vol., no., pp.1825,1832, 21-25 Feb. 2010

[10] Toshihiro Keishima, Akira Kataoka, Izuo Hirota, "Induction cooker with heating coil and electrical conductor". Patent US7049563 B2. filed May 23, 2004. published May 23, 2006.

[11] Koertzen, H.W.; Van Wyk, J.D.; Ferreira, J.A., "Design of the half-bridge, series resonant converter for induction cooking," *Power Electronics Specialists Conference, 1995. PESC '95 Record., 26th Annual IEEE* , vol.2, no., pp.729,735 vol.2, 18-22 Jun 1995

[12] Hirota, I.; Omori, H.; Nakaoka, M., "Performance evaluations of single-ended quasi-load resonant inverter incorporating advanced-2nd generation IGBT for soft switching," *Industrial Electronics, Control, Instrumentation, and Automation, 1992. Power Electronics and Motion Control., Proceedings of the 1992 International Conference on* , vol., no., pp.223,228 vol.1, 9-13 Nov 1992

[13] Shenkman, A.; Axelrod, B.; Berkovich, Y., "Single-switch AC-AC converter with high power factor and soft commutation for induction heating applications," *Electric Power Applications, IEE Proceedings* - , vol.148, no.6, pp.469,474, Nov 2001

[14] Ogiwara, H.; Itoi, M.; Nakaoka, M., "PWM-controlled soft-switching SEPP high-frequency inverter for induction-heating applications," *Electric Power Applications, IEE Proceedings* - , vol.151, no.4, pp.404,413, 7 July 2004

[15] Ahmed, N.A.; Eid, A.; Hyun Woo Lee; Nakaoka, M.; Miura, Y.; Ahmed, T.; Hiraki, E., "Quasi-Resonant Dual Mode Soft Switching PWM and PDM High-Frequency Inverter with IH Load Resonant Tank," *Power Electronics Specialists Conference, 2005. PESC '05. IEEE 36th* , vol., no., pp.2830,2835, 16-16 June 2005

[16] Saha, B.; Rae-Young Kim, "High Power Density Series Resonant Inverter Using an Auxiliary Switched Capacitor Cell for Induction Heating Applications," *Power Electronics, IEEE Transactions on* , vol.29, no.4, pp.1909,1918, April 2014

[17] Sarnago, H.; Lucía, O.; Mediano, A.; Burdío, J.M., "Class-D/DE Dual-Mode-Operation Resonant Converter for Improved-Efficiency Domestic Induction Heating System," *Power Electronics, IEEE Transactions on* , vol.28, no.3, pp.1274,1285, March 2013

[18] Sarnago, H.; Lucia, O.; Mediano, A.; Burdio, J.M., "Dual-mode-operation half-bridge resonant converter for improved-efficiency induction heating system," *Applied Power Electronics Conference and Exposition (APEC), 2012 Twenty-Seventh Annual IEEE* , vol., no., pp.2184,2188, 5-9 Feb. 2012

[19] Saha, B.; Hyun Woo Lee; Nakaoka, M., "Utility Frequency AC to High Frequency AC Power Converter with Boost-Half Bridge Single Stage Circuit Topology," *Industrial Technology, 2006. ICIT 2006. IEEE International Conference on* , vol., no., pp.1430,1435, 15-17 Dec. 2006

[20] Saoudi, M.; Puyal, D.; Bernal, C.; Anton, D.; Mediano, A., "Induction cooking systems with single switch inverter using new driving techniques," *Industrial Electronics (ISIE), 2010 IEEE International Symposium on* , vol., no., pp.878,883, 4-7 July 2010

[21] Nishida, T.; Gamage, L.; Muraoka, H.; Hiraki, E.; Nakaoka, M.; Kifune, H.; Hatanaka, Y.; Hyun-Woo Lee, "Cost effective soft-switching PWM high frequency inverter with minimum circuit components for consumer induction heater," *Power Electronics Specialist Conference, 2003. PESC '03. 2003 IEEE 34th Annual* , vol.4, no., pp.2015,2020 vol.4, 15-19 June 2003

[22] Ogura, K.; Gamage, L.; Ahmed, T.; Nakaoka, M.; Hirota, I.; Yamashita, H.; Omori, H., "Performance evaluation of edge-resonant ZVS-PWM high-frequency inverter using trench-gate IGBTs for consumer induction cooking heater," *Electric Power Applications, IEE Proceedings* - , vol.151, no.5, pp.563,568, 9 Sept. 2004

[23] Saha, B.; Soon Kurl Kwon; Ahmed, N.A.; Omori, H.; Nakaoka, M., "Commercial Frequency AC to High Frequency AC Converter With Boost-Active Clamp Bridge Single Stage ZVS-PWM Inverter," *Power Electronics, IEEE Transactions on* , vol.23, no.1, pp.412,419, Jan. 2008

[24] Sugimura, H.; Saha, B.; Sumiyoshi, S.; Omori, H.; Sang-Pil Mun; Soon-Kurl Kwon; Hiraki, E.; Nakaoka, M., "New Built-In Induction Heating Cooker Using High-Frequency ZVS-PWM Converter with Single Stage Circuit Topology," *Industry Applications Society Annual Meeting, 2008. IAS '08. IEEE* , vol., no., pp.1,6, 5-9 Oct. 2008

[25] Nishida, T.; Moisseev, S.; Hiraki, E.; Nakaoka, M., "Duty cycle controlled soft commutation high frequency inverter for consumer induction cooker and steamer," *Industrial Electronics Society, 2003. IECON '03. The 29th Annual Conference of the IEEE* , vol.2, no., pp.1846,1851 Vol.2, 2-6 Nov. 2003

[26] Kawaguchi, Y.; Hiraki, E.; Tanaka, T.; Nakaoka, M., "Full bridge phase-shifted soft switching high-frequency inverter with boost PFC function for induction heating system," *Power Electronics and Applications, 2007 European Conference on* , vol., no., pp.1,8, 2-5 Sept. 2007

[27] Kawaguchi, Y.; Hiraki, E.; Tanaka, T.; Nakaoka, M.; Fujita, A.; Omori, H., "Feasible evaluation of a full-bridge inverter for induction heating cooking appliances with discontinuous current mode PFC control," *Power Electronics Specialists Conference, 2008. PESC 2008. IEEE* , vol., no., pp.2948,2953, 15-19 June 2008